Ph.D Thesis

A Study of Recognizing Flake Surfaces of Stone Tool Based on Feature Lines Extracted by Mahalanobis Distance Metric

Shurentsetseg Erdenebayar

Department of Design and Media Technology
Graduate School of Engineering
Iwate University

September 2019

Abstract

One of the areas that benefit from point clouds is cultural heritage research. The study of point clouds is contributing to cultural heritage saving for the next generation. One example is the study of stone tool. The study of stone tools plays an increasingly important role in the behavior of our ancestors. The surface collection obtained from excavated stone tools required to be open for archaeological research. In this purpose, the publication of the stone tool study needs to be presented. Archaeological research is commonly used stone tool illustration which is called "Scale drawing". Drawing a scale drawing is too time-consuming work. Reassembling Fractured Objects is the important concept of technological analysis of stone tool artifacts. In general, the problem of matching real-world archaeological fragments is a complex and time-consuming task. Because the evaluation of similarity between artifacts and their parts is difficult to evaluate. To facilitate the time-consuming work of scale drawing and matching of fragmented objects, this thesis studied computer graphics techniques to assist the study of stone tools. The thesis mostly considers the two aspects about extracting feature line and recognizing flake surfaces.

In archaeological research, the scale drawing, which is hand-drawn from measured stone tools, is traditionally used. In the scale drawing creation, a base drawing which consists outline and ridge lines is initially drawn from geometric features of shape. After that other lines are extracted from knowledge of making stone tools and are added to the base drawing. It requires special knowledge to extract feature lines from stone tools so that scale drawing is time-consuming. Therefore, if the base drawing is automatically extracted, the working hours are reduced. To overcome this issue, this paper proposes a feature line extraction method using the Mahalanobis distance metric. First,

the points on the outline are extracted from a point cloud. Then, the surface variation is calculated with a various number of neighbors and thus the potential feature points are detected by the analysis of its surface variation. After that, the potential feature points are thinned towards the highest variation points by using Laplacian smoothing. Then, the thinned feature points are shrunk to the potential feature points. Finally, a feature line is extracted by connecting the nearest thinned feature points locating in the Mahalanobis distance field. To verify our method, the extracted outline and ridge lines are compared to scale drawing of the stone tool drawn by archaeological illustrators. Our method is applied to stone tools, and we confirm the effectiveness of our method.

Studying stone tools provides us with information about the human history dating as far back as 2.5 million years ago. Nowadays, the important historic artifacts of stone tools are studied by functionality and technological analysis of lithic analysis. The reassembly process of stone tools is commonly done in lithic materials. The reassembly process can be easily done by the refitted flake matching process. The refitted flake matching process is required for highly accurate segmented flakes. The thesis presents an algorithm for automatic recognition of the flake surface based on feature lines of stone tools from point clouds. The feature-line-based recognition method for the flake surface is very effective for stone tools because it is based on the geometric characteristic of stone tools. The proposed segmentation method is based on the seeded-region method. Before the segmentation, surface normal at a point is estimated from neighbor points and the nearest distance from a point to feature line segment is calculated. Initially, the furthest point from the feature line is selected for a seed point. Then, the seed point clusters its neighbor points by the following two criteria. First, neighbor points of seed point are calculated. To save the program processing speed, a distance threshold is used. If the distance of a selected neighbor point is greater than a given threshold value, the neighbor point is clustered to the seed point region. Second, if the neighbor point is located near the feature line, the local coordinate system is constructed along the normal vector of the seed point. Then, a line is constructed by seed point and its neighbor point. If the line does not intersect with the nearest feature line segment on the local coordinate system, the neighbor point is segmented into the seed point region. If line segments intersect with each other on the local coordinate system, the neighbor point is selected to a new seed point

and the new region is created. The extracted flakes are compared to other segmentation methods. The implementation of this work can recognize flake surfaces according to the scale drawing of the stone tool with high accuracy.

This thesis presents an algorithm of automatic recognition of flake surfaces from point clouds. The proposed flake surface recognizing method is very effective for stone tool analysis because the proposed method is based on the fundamental characteristic of stone tools. 3D model of lithic material is tested. The proposed method is compared with different segmentation method. Mahalanobis distance metric is used to extract candidate points of feature lines. The extracted feature line is compared to a scale drawing of the stone tool drawn by archaeological illustrators. In the result, the flake surface can be efficiently recognized. The limitation of the proposed method has been solved in future work.

Acknowledgements

First, I would like to express my sincere gratitude to the head of the National University of Mongolia, my honoured professors and colleagues. I am also grateful to the team of "M-JEED 1000 ENGINEERS" higher engineering education development project.

Foremost, I deeply thank my honoured supervisor Prof.Kouichi Konno. This thesis would not have been possible without your support and guidance. I am very grateful for your advice and inspiration for me these past three years. Thank you for all that you have done for me. My sincere thanks also goes to associate Prof. Enkhbayar Altantsetseg, who provided me with an opportunity to meet my supervisor Prof. Kouichi Konno, and who supported me to study in abroad. Without your precious support, I would not have started this research. I am indebted to Batjargal Sosorbaram. Thank you for your unwavering optimism and energy during my days of uncertainty.

Besides my advisor, I would like to thank the rest of my thesis committee: Prof. Tadahiro Fujimoto and Prof.Takamitsu Tanaka, for their insightful comments and encouragement, but also for the hard question which incented me to widen my research from various perspectives.

I am also grateful to the Iwate University staff. A special thank to Mrs Hikaru Kakeda. Your warm friendship made me always happy. Thanks also to the members of Konno-Matsuyama Laboratory. Thank members of Lang LANG CO., LTD for yours accompany. Part of this work was supported by JSPS KAKENHI Grant Number JP18H00734.

Last but not least, I would like to express my deepest gratitude to my family and friends. This dissertation would not have been possible without their warm love, continued patience, and endless support. A big loving thank you to my husband, especially for encouraging me when I had a trouble. This thesis would never have finished without your support and hospitality.

Contents

List of Figures

List of Tables

Chapter 1

Introduction

1.1 Overview of The Chapter

This chapter mainly introduces lithic analysis and key understanding of this study. Moreover, the problem statement for recognizing flake surfaces and creating a scale drawing is reported.

1.2 Background

In recent years, high-resolution cameras and laser scanners [28] have developed for various researches and industries. 3D scanners measure a large number of points on the external surfaces of objects around them. According to these devices, real objects of any size can be converted into three-dimensional digital data called a Point cloud [19]. Technically a point cloud is a database containing points in the three-dimensional coordinate system. The point cloud is an accurate digital record of an object or space with accuracy in the range of 0.1 mm or better. It is saved in the form of a very large number of points that cover surfaces of a sensed object. Point clouds are used to create three-dimensional models used in various fields including medical imaging, architecture, three-dimensional printing, manufacturing, three-dimensional gaming and various virtual reality (VR) applications. One of the areas that benefit from point clouds is cultural heritage research. Three-dimensional point cloud processing

Figure 1.1: Stone tools [37]

can restore archaeological and cultural heritage efficiently. One example is to assist the study of stone tools.

Stone tools are valuable archaeological findings and are the important historical artifacts of humanity. Study of stone tools illustrates among the unique features of the lives and evolution of hominins. The study of stone tools plays an increasingly important role in the behavior of our ancestors [35]. Stone tools made around three million years ago are common and diverse in the world. Stone tools consist mainly of stone and bone tools. They reflect a wide range of manufacturing techniques and tool-using activities [36]. Behalf of the production, stone tools have occasionally to deal with other stone tools as well. Figure 1.1 shows the stone tools used in the Jomon period of Japan. The Jomon Period is the earliest historical era of Japanese history. The end of the Ice Age coincided with the closure of the Paleolithic era when stone tools were used as main instruments, and thus the Jomon period began approximately 13,000 years B.C. The prehistoric culture that flourished at that time is called the Jomon culture.

The study of stone tools and stone tool technology is called lithic analysis. In the lithic analysis, archaeological material was produced through lithic reduction (knapping) or ground stone. The earliest known stone tools [43] are assigned to the Oldowan Industry and consist of sharp stone flakes struck from cobble cores by direct percussion with another stone (the "hammer stone") [45]. In the result, flake pieces with various size and a core stone are produced. The manufacturing process is shown in Figure 1.2. These pieces are called lithic materials. The left rock from an original raw material is a core and peeled piece fitted to the core is a flake surface /flake scars/ [31]. The lithic materials represent much of our earliest evidence for human behavior. In the lithic analysis, artifacts of stones tools are usually analyzed by typological analysis, functional analysis, and technological analysis [1].

In archaeology, a typology is the result of the classification of things according to their physical characteristics. Typological classification is the act of artifact classification based on morphological similarities. Resultant classes include those artifacts subsumed by a tool, production, and debitage categories.

Functional analysis of stone tools is a variety of approaches designed with the aim of identifying the use of a stone tool. Functional analysis of stone tools is based on the argument that the uses to which tools were put in antiquity leave diagnostic damage and/or polish on their working edges. This type of analysis is also known as use-wear analysis.

The technological analysis studies the important concepts of stone tool technology. Technological analysis is concerned with the examination of the production of knapped-stone artifacts. Technological analysts identify flake scarring on stone artifacts in order to understand the manufacturing process of flake production. There have been efforts to identify variables to predict the original size of discarded tool artifact. To predict the original size, the various proportions of an assemblages flake sizes are compared. A very wide range of attributes may be used to characterize and compare assemblages to isolate (and interpret) differences across time and space in the production of stone tools.

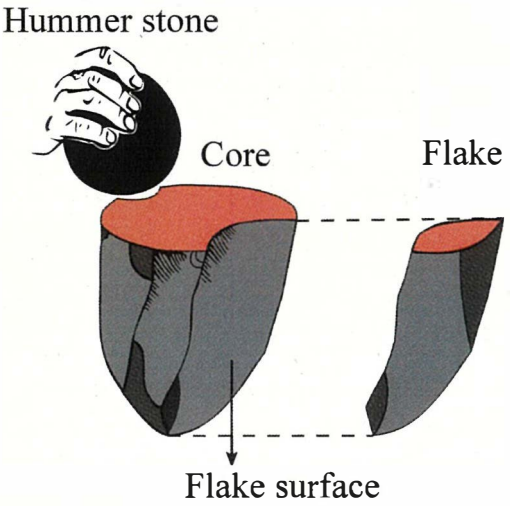

Figure 1.2: Manufacturing of stone tools.

Figure 1.3: Excavated flake pieces.

1.3 Problem Statement

According to technological studies, application for the assembling of lithic materials (artifacts made from rocks or minerals) is very important for lithic analysis. For instance, to define how were stone tools made, some lithic materials need to be assembled as a single piece of stone. Moreover, excavated lithic materials are obtained commonly in fractured style due to the long-time storage of million year. Thus, the broken fractured pieces also need to be assembled. The reassembly process of flake surfaces is an important concept in the lithic study. The reassembly process of stone tools can be easily done by the refitted flake matching process. But the matching and reassembling of lithic materials are the hard task for archaeologists in massive data. For example, there just is not that much potential for variation in Oldowan flake production. It is only with more complicated technologies that multiple variants become possible because more choices are possible [45]. Figure 1.3 shows the excavated flake pieces needed to reassemble.

The refitted flake matching process is required for highly accurate segmented flakes. The thesis presents an algorithm for automatic recognition of the flake surface based on feature lines of stone tools from point clouds. Our work is focused on recognizing flake surfaces using feature lines extracted like a scale drawing of the stone tool. The scale drawing is an essential study of stone tool research. It can provide important information about lithic materials and detailed in Section 1.4. The proposed feature-line-based recognition

method for the flake surface is very effective for stone tools because it is based on the geometrical and archaeological properties of the stone tool.

This research refers to two main topics feature line extraction of stone tools and recognizing flake surfaces of stone tools. To simplify the time-consuming work of scale drawing, this thesis proposed a new method of extracting feature lines for stone tools using the Mahalanobis distance metric. Moreover, to accurately recognize flake surfaces, this thesis introduces feature-line-based segmentation method.

1.4 Research Method

In the archaeological application of stone tools, the scale drawing, which is hand-drawn from measured stone tools, is traditionally used. It is generally used in the excavation report in the archaeology area. To publish an excavation report, archaeologists measure stone tools and then make scale drawings by manual operations.

The scale drawing is an archaeological illustration and not a perspective figure. Because of including surface information, it does not look like the drawing object. It can create collaboration between the illustrator and the lithic specialist. Usually, a single lithic artifact may have several surfaces and each surface requires separate stylistic treatment in an archaeological application. For example, there may be natural fractures resulting from burning or freeze-thaw climatic conditions, which must be distinguished on the drawing from humanly produced facets. To be able to indicate the humanly struck areas on worked flint, which are normally apparent as negative flake beds or scars, it is essential to understand the direction of each flake removal. Flint fractures conchoidally, that is in a manner resembling the curved, concentrically ribbed surface of some shells [2]. In other words, from the point of impact where the hammer strikes the flint surface, a series of concentric ripples are formed which are often visible both on the bulbar surface of the struck flake and on the negative flake scar left on the core or implement being worked. These ripples must be recorded to indicate the direction of flaking involved, and are usually drawn in continuous curved lines "rings" shown in Figure 1.4. In practice, wealthy information about physical properties is illustrated by the various curves in the scale drawing. With these curves, important sources

of information such as flake surface. the oriented direction of strike and the sequence of strikes are included in a scale drawing.

Scale drawing is a systematic drawing and it must follow certain procedures of drawing [2]. The procedure to illustrate a scale drawing is to use two-dimensional images to provide an intelligible description of a three-dimensional object.

In general, scale drawing is represented by four elements, such as outlines, ridge lines, rings, and fissures [24]. Outlines and ridge lines can be extracted from geometric features of the shapes. Rings and fissures have to be investigated from precise observation of specialists and extracted on the knowledge of making stone tools. In the scale drawing creation, a base drawing which consists outline and ridge lines is initially drawn from geometric features of shape. After that other lines are extracted from knowledge of making stone tools and are added to the base drawing. It requires special knowledge to extract lines from stone tools so that scale drawing is time-consuming. Therefore, if the base drawing is automatically extracted, the working hours are reduced. To overcome this issue, this thesis proposes a feature line extraction method using the Mahalanobis distance metric using computer graphics.

In computer graphics, the scale drawing and base drawing are illustrated by feature lines. Extracting feature line is an important process in computer graphics and point cloud processing. A feature line represents an object in the drawing as a valley or a ridge line. A feature line is a special type of line that can be used to segment and recognize the object.

Figure 1.4 (a) shows an example of scale drawing from the front, side and back, done by a lithic specialists [3]. Figure 1.4 (b) shows the steps of making a scale drawing of the stone viewed from the front. First, the specialist allocates a drawing area. The longitudinal of a stone tool is drawn along the vertical axis. After that outlines are measured and marked in the sketch. Then outlines are drawn by tracing the measured points. After finishing the outlines, the points on the ridge lines are measured and plotted in the sketch. These points are traced in the same manner. In this thesis, the illustration of outline and ridge line calls base drawing. Finally, rings and fissures are added to the base drawing. Making scale drawings from hundreds of stone tools is quite time-consuming. Therefore, efficiency methods are required to reduce time consumption by using point clouds. Outlines and ridge lines are clearer to be extracted and compared to the rings and fissures because these lines are

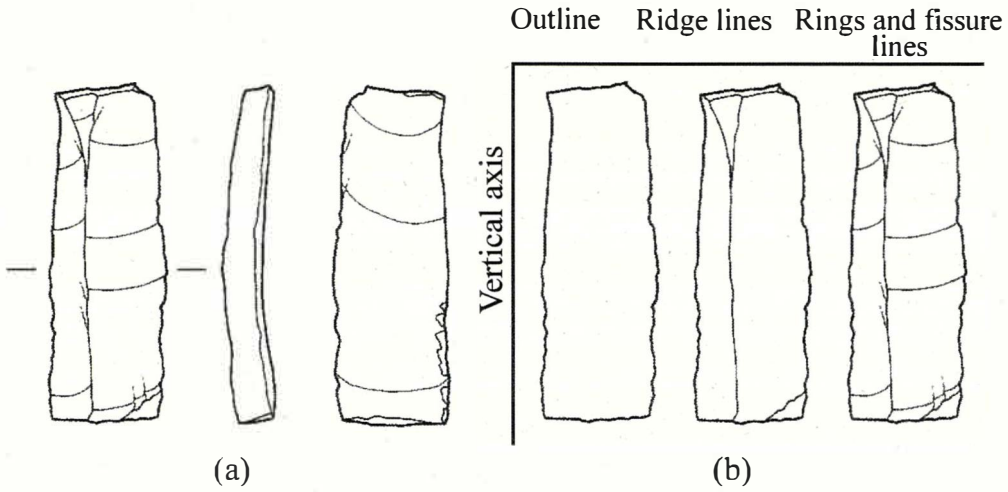

Figure 1.4: (a) An example of manual scale drawing [3], (b) an example of the steps of the scale drawing

geometric features. On the other hand, to extract rings and fissures require special knowledge of archaeology. Therefore, if outlines and ridge lines are extracted and base drawing is automatically generated, the creation time of scale drawing becomes compressed. Our work aims to extract automatically generate base drawing to simplify time-consuming work of making a scale drawing.

A flake surface is defined by the closed area which is bounded by ridge line. Therefore, all of the flake surfaces are represented by the closed line sequence into the base drawing even if the geometric shape of the ridge line may be an ambiguous shape.

There are several techniques to extract feature lines from point clouds [14, 15, 16, 20, 38], while they cannot sufficiently extract feature lines like scale drawing. [16, 20] compute the minimum spanning tree to extract feature lines. Their technique is capable of extracting feature lines by connecting existing feature points. Therefore, if the point cloud has any noise, it can get a robust and accurate result. Since a stone tool contains ambiguous shape, closing of flake surface boundary and finding the connection point may be difficult. Therefore, the feature lines to make a base drawing are not sufficiently extracted. Because of the complication, a simple and efficient technique is required.

In this research, a novel feature line extraction method which is expanded by [8] is proposed. The proposed method introduces more flexible distance metric to extract feature lines for a base drawing creation automatically. Our algorithm selects candidate points on feature lines using its dependence on neighbor propagation. Feature lines extracted from a point cloud are evaluated by comparing with for technical hand drawing and we verify our method has effectiveness.

To facilitate time-consumption work of base drawing, this thesis proposed for extracting feature line using Mahalanobis distance metric. Therefore, to improve the matching process, this thesis proposed for recognizing flake surfaces using extracted feature lines. Most of the stone tools illustrated and described in this thesis were made in Joman periods of Japan. Three-dimensional models of sampled stone tools are tested, in order to improve recognizing the flake surfaces. The experiment result shows the effectiveness of our proposed method.

1.5 Organization of The Thesis

This thesis is composed of 5 chapters including this chapter and every chapter is composed of several sections. The thesis is arranged as follows:

Chapter 1 provides background information and an essential concept of the study of the stone tool. It also states key findings of this thesis and poses a brief introduction to our main contribution.

Chapter 2 introduced the related work of recognizing flake surfaces and the computer graphics techniques used in the lithic analysis. A 3D surface reconstruction technique using a four-directional measurement machine is introduced. Moreover, a Mahalanobis distance metric for a point cloud and the previous work for constructing a feature line are introduced.

In Chapter 3, the proposed feature point and feature line detection algorithm based on Mahalanobis distance are initially introduced. Additionally, a new evaluation method is presented. Furthermore, the evaluation result and extracted feature lines are shown.

In Chapter 4, the novel feature-line-based segmentation method is introduced. Sample stone tools are tested. Moreover, recognized flake surfaces are compared to another segmentation method.

Chapter 5 summarized our work of recognizing flake surfaces and suggested future research.

Chapter 2

Related Works

2.1 Overview of The Chapter

This chapter first introduces the 3D surface reconstruction technique using a four-directional measurement machine. Then, the previous study of feature line extraction is introduced. Next, the Mahalanobis distance metric for a point cloud is introduced. After that, the related works of matching and recognizing flake surfaces are introduced. Finally, the computer graphics technique used in the lithic analysis is introduced.

2.2 Data Acquisition

Our data are acquired from a 3D surface reconstruction technique using the four-directional measurement machine developed by Iwate University and LANG Co., Ltd. [6, 12]. Hundreds of stone tools can be scanned at the same time and the surface feature is intact preserved, such as sharp edges, flake scars, benefiting from the highest 0.1 mm precision of laser scanner. Additionally, the stone tools are from archaeological researchers in the university and the Buried Cultural Property Investigation Center which we cooperated with. In the actual data, there are some holes need to be filled manually, and some data are not registered very well.

Figure 2.1: Scanning Device.

2.3 Previous Study for Extracting Features

Feature line construction is a difficult task for stone tools. Recently many approaches have been proposed [7, 53]. What edges are extracted to a feature line is a difficult question for feature line extraction of the stone tool because of the ambiguous shape of the edges. Therefore, additional conditions are required.

Lin et al. [29] proposed the feature line extraction method with a closed frame structure for a stone tool. At first, the local coordinate with the PCA algorithm is calculated and the polynomial equation is fitted with moving least-squares (MLS) theory. The curvature of each point is estimated with the polynomial fitting method. Second, potential feature points are detected by the mean curvature. Third, potential feature points are classified to inner and outer potential feature points. Next, selected potential feature points are thinned by Gaussian smoothing. After that, the densely-located feature points are clustered with the Euclidean minimum spanning tree (EMST) algorithm. The potential feature points are constructed by the EMST algorithm. Through the result of the EMST algorithm, noise nodes can be removed, and the longest feature line can be connected with the node valence of the EMST. Finally, the inner feature line is stitched by the outer feature line with a threshold. In the result, the closed frame structure of stone tools is constructed.

Using an EMST to construct feature lines has an advantage of reducing time complexity. But the longest lines will be strongly influenced than the curvature of point for constructing feature lines. As a result, the error between the constructed feature line and scale drawing of the sampled stone tool is high. The reason is that points on the sharp edges have high curvature.

In the previous work, we aim to extract ridge lines of the stone tool automatically. In this purpose, firstly every point is evaluated by using the principal curvature. If a mean curvature is greater than the given threshold value, it is selected as a potential feature point. Then, potential feature points are thinned by the Gaussian filter. The thinning feature points are smoothed and reduced by using Laplacian smoothing. The feature line is extracted by connecting the nearest feature points with Euclidean distance. But the result of the extracted feature line is not sufficient to illustrate for the stone tool.

This algorithm has several limitations. The first limitation is a single threshold value is used to detect entire feature points, the significant feature points of the feature line are not detected. The second limitation is Gaussian smoothing takes a lot of time and greatly affects to point location. The third limitation is connecting feature lines needs an additional condition.

The scale drawing is an archaeological drawing. Thus precise edge points are important to illustration. Moreover, a precise construction method of feature lines needs to be introduced. This thesis introduced a Mahalanobis distance metric in point clouds.

Feature extraction methods for the point cloud have been introduced over the past two decades. Generally, the entire process of feature line extraction consists of two main concepts; to extract feature points and to connect the feature points. About feature extraction, Daniels et al. [14] first introduced two kinds of the division for feature extraction methods: point-based and triangle mesh-based. According to the methodology, our algorithm belongs to a point-based method because the curvature of points is directly detected from the unorganized point clouds.

Gumhold et al. [20] first formulated curvature using PCA (Principal Component Analysis) for point clouds. The eigenvectors of PCA are used to divide the potential points into the boundary points, points on the edge, and corner points. Eventually, the minimum spanning tree (MST) is used to construct feature lines. Daniels et al. [15, 18] detected feature points using locally fitting robust moving least-squares polynomials and then projected these points onto the intersections of multiple surfaces to obtain feature lines. The major advantage of the method is that it can work properly in the condition of noisy unorganized points and the output feature line is smooth and complete because it extracts feature curves on the reconstructed moving least squares (MLS) surface.

Demarsin et al. [16] segmented point clouds into several groups based on the normal variation in local neighborhoods. The region of a sharp edge is identified by high variation of normals. Also, they use the region growing algorithm, and to build sharp feature line, they used a minimum spanning tree constructed between the boundary points of the classified clusters.

Except for the time complexity, Kalogerakis et al. [23] estimated curvatures accurately using the surface normal. Weber et al. [47] extracted

sharp features of point-sampled geometry using Gauss map clustering on local neighborhood points. However, that method did not make sense on smooth features. Pang et al. [38] used to fit local quadric surfaces in order to estimate curvatures, and valley and ridge lines were grown by a maximum and minimum principal curvature. Kim [25] computed a local Voronoi diagram to obtain neighborhood information and used the moving least square method to calculate local curvatures. However, the Voronoi map is sensitive to outliers. Enkhbayar et al. [8] expanded spectral analysis, and they successfully approached the Fast Fourier Transform to estimate the curvature of a point cloud. Then, feature points can be detected by the principal curvature.

The studies in [15, 38] use projection-based method for extracting features from detected potential feature points. In [14], potential feature points are projected to the intersections of locally fitted surfaces. After smoothing projected points, polylines are grown through the projected points. Feature points are smoothed in [8] by projecting them onto their principal axis of neighborhoods. Pauly et al. [41, 40] accomplished multi-scale PCA on a point cloud by using an adaptive number of neighborhood points. Due to the varying shape of stone tools, a variation of each dimension is suitable to detect potential feature points by using multi-scale PCA. [41, 20, 16] used a minimum spanning tree to construct feature lines. Enkhbayar et al. [8] introduced a line growing technique to construct feature lines. All of those techniques are calculated in Euclidean space.

The Euclidean distance function is useful for a continuous space where all dimensions are properly scaled and relevant. However, the shape of a stone tool has a complicated structure. As our data, oval and oblong stone tools are the common feature. Therefore, the feature points of stone tools are usually detected lined-up and the detected local feature points usually have a strong correlation. The feature line extraction from stone tools [8, 20] by connecting potential feature points is a difficult task. [8] shows the feature line extraction of stone tools, but feature lines could not be easily extracted from the detected points for some stone tools.

A novel way to look into this issue is to take advantage of a more flexible metric due to increased requirements. This work proposes new algorithms to detect the feature lines constructing points that are propagated in the most standard deviations using the Mahalanobis distance metric. Using the nearest distance of Mahalanobis, it is advantageous to extract a precise feature

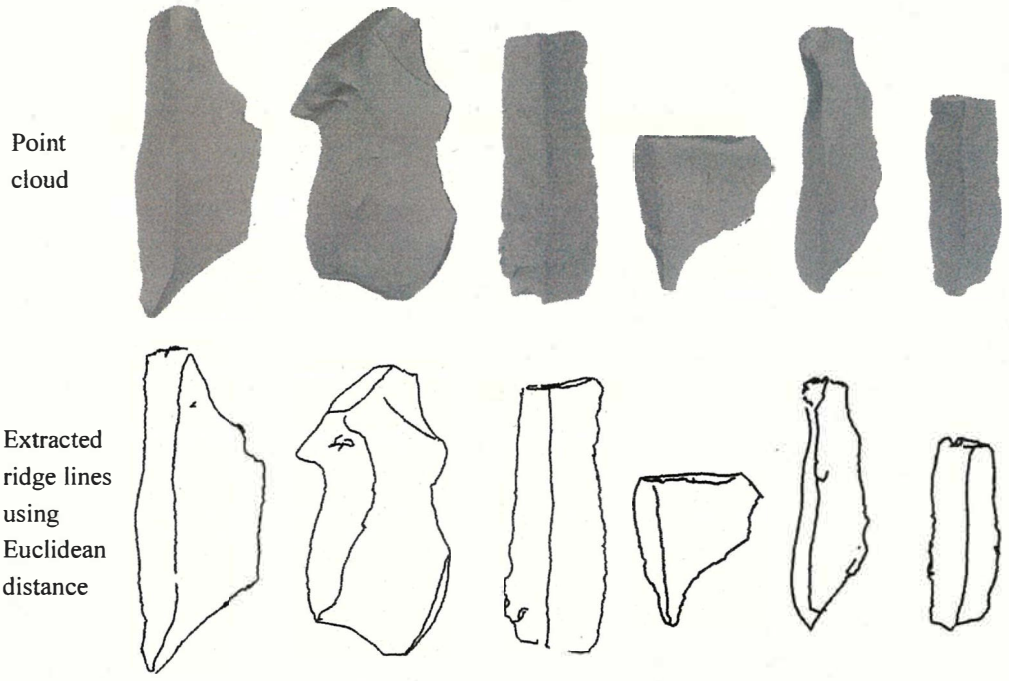

Figure 2.2: Point cloud of stone tools [3] and result of ridge line extraction [8].

line compared with a Euclidean distance metric. In general, the Mahalanobis distance metric is fit for large margin data and usually used in image processing and machine learning. Moreover, geometrically, the Mahalanobis distance metric can adapt the geometrical distribution of data so that the distance between similar data points is small [50]. Therefore, it can improve the performance of clustering or classification algorithms, such as k-nearest neighbor (KNN) classifier. Such advantages can be used to perform special tasks on a given data set if a suitable Mahalanobis distance metric is given. For instance, Xiang et al. [49] use it for data clustering and classification.

Euclidean distance represents the distance between two points. Hence it represents a physical distance between two points. For example, if distance metric is a Euclidean distance for performing K-means clustering, points belong to the same cluster but they have opposite directions since the distance of these points from the centroid is the same and Euclidean distance not related to principal direction. In recent years, there are a lot of papers published for extracting feature lines [27, 21, 33]. Line construction method using angle threshold value is not adaptive for k-nearest neighbor points. Hence this

method is not a good fit for some stone tools. Because of this issue, a new distance metric method based on Mahalanobis distance metric is introduced.

In the base drawing, the ridge lines are drawn along the longest sharp edges of stone tools. The detected feature points of such edges have high variation. Therefore, longitudinal connecting along the edges is the best optimization to create the base drawing. Feature points cannot be easily connected depending on the variation, because Euclidean distance considers all dimensions have the same variation. Another disadvantage is if there is no feature point to grow in a certain distance, [41, 20, 16] cannot sufficiently construct feature lines. Increasing the connecting radius is not optimal for modifying the feature lines. Figure 2.2 shows the result of ridge line extraction [8] with principal curvature [17]. When using Euclidean distance, lines cannot be sufficiently extracted and there are gaps between lines.

Today semi-automated illustration system PEAKIT [11] which is used in the archaeological application has introduced in markets. It creates an image illustrating both geometric and archaeological features of stone tools. First features are extracted by openness [11]. Then, extracted features are traced by manual operation. Therefore, PEAKIT system still has time complexity. If outlines and ridge lines are extracted and base drawing is automatically generated, the creation time of scale drawing becomes compressed.

2.4 A Mahalanobis Distance Metric for Point Clouds

The connection of feature points is hardly required to make a closed area for base drawing creation. For this purpose, our research introduces a Mahalanobis distance metric for constructing feature lines.

Euclidean distance is the commonly used straight line distance between two points. Euclidean distance will work fine as long as the dimensions are equally weighted and are independent of each other. If the dimensions are correlated to one another, the Euclidean distance between a point and the center of the points (distribution) can give little or misleading information about how close a point really is to the cluster. In Figure 2.3 (a), the two points above are equally distant from the center in Euclidean distance. Technically

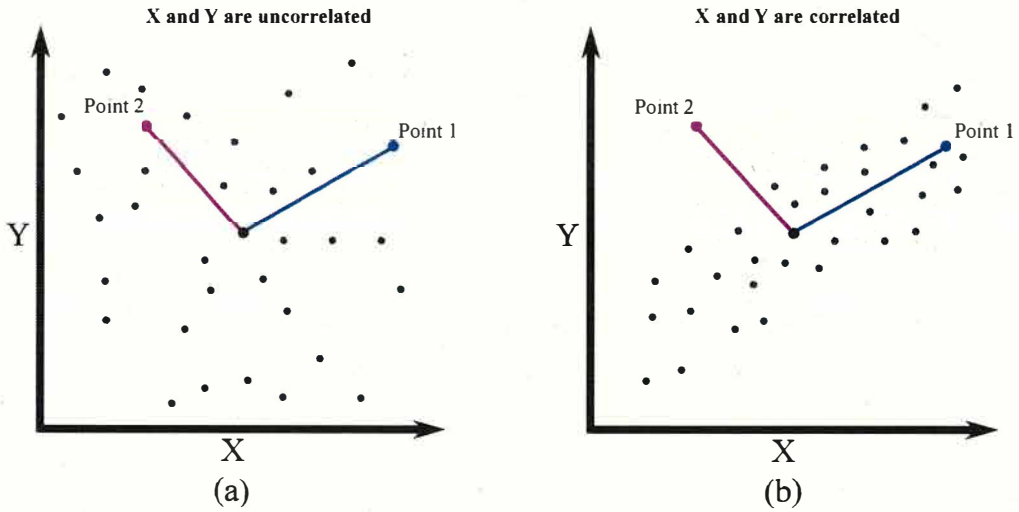

Figure 2.3: The types of a scatterplot of variables

the Euclidean distance between the two points is equal. Because Euclidean distance is a distance between two points only. It does not consider how the rest of the points in the dataset vary. Therefore, it cannot be used to really judge how close a point actually is to the distribution of points. Figure 2.3 (b) is a simple scatterplot of two variables that are positively correlated with each other. That is, as the value of one variable (x-axis) increases, so does the value of the other variable (y-axis). What we need here is a more robust distance metric that is an accurate representation of how distant a point is from a distribution.

Mahalanobis distance is the distance between a point and a distribution. It is not a distance between two distinct points. It was introduced by Prof. P. C. Mahalanobis in 1936 and has been used in various statistical applications ever since. Mahalanobis distance measure takes into account correlations between attributes by which different patterns can be identified and analyzed as it is computed using the inverse of the variance-covariance matrix of the data set [4].

The Mahalanobis distance of a multivariate vector $x = (x_1, x_2, x_3, ..., x_N)^T$ from the values of a group with mean $\mu = (\mu_1, \mu_2, \mu_3, ..., \mu_N)^T$ and covariance matrix S, is defined as:

$$D_M(x) = \sqrt{(x - \mu)^T S^{-1} (x - \mu)} \tag{2.1}$$

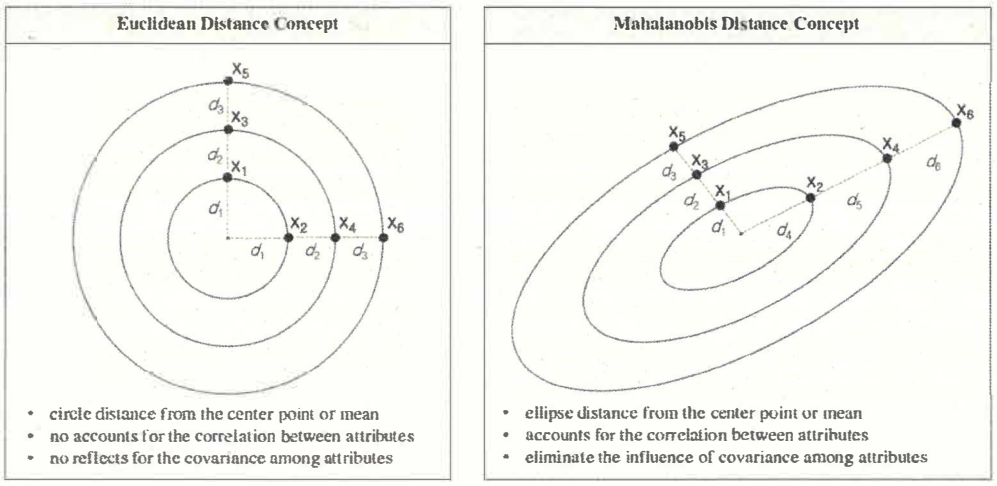

Figure 2.4: Comparison of the Mahalanobis distance and Euclidean distance [4]

A crucial difference from Euclidean distance is that Mahalanobis distance considers the correlations of the data set. The Mahalanobis distance is affected by both variance and correlation. If the covariance matrix is the identity matrix, then it is the same as the Euclidean distance. If the covariance matrix is diagonal, then it is called the normalized Euclidean distance [4].

Figure 2.4 compares the Mahalanobis and Euclidean distance methods. The characteristics of the Mahalanobis distance can be summarized as 1) reflecting the variances in each direction being different, 2) accounting for the covariance between attributes, and 3) reducing to the familiar Euclidean distance for uncorrelated attributes with unit variance [4].

The Mahalanobis distance metric estimates a distance between two feature points in space for their relevant features. Units in each direction are different because variances in each direction are different. The distribution of points which located the same distance from the center point has a circular or spherical shape in the Euclidean distance metric. Whereas the distribution of points which located the same distance from the center point has ellipse or ellipsoid in the Mahalanobis distance metric, depending on the distribution of the nearby points. Therefore, connecting feature points along the major axis of an ellipse is efficient to extract closed ridge lines. This study proposes a feature line extraction method of stone tools using Mahalanobis distance metric in order to generate the base drawing.

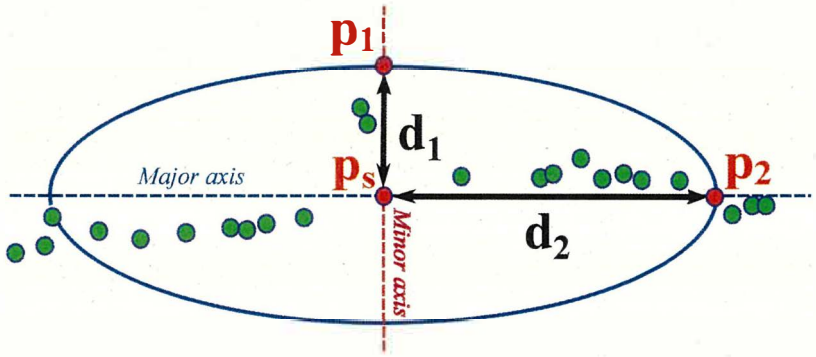

Figure 2.5: Mahalanobis distance measure

Figure 2.5 shows the Mahalanobis distance measure. The ellipse is shown in Figure 2.5 presents the distribution shape of points which are located the same distance from the center point in the Mahalanobis distance metric. In Figure 2.5, selected point $\mathbf{p}_s$ and its nearest neighbor points $\mathbf{p}_1$ and $\mathbf{p}_2$ are described. According to the Euclidean distance metric, the $\mathbf{p}_2$ is located far from the $\mathbf{p}_s$ compared to the $\mathbf{p}_1$. However, according to the Mahalanobis distance metric, the $\mathbf{p}_1$ and $\mathbf{p}_2$ is located same distance from the $\mathbf{p}_s$.

Given two data points $\mathbf{p}_i$ and $\mathbf{p}_j$, the Mahalanobis distance can be calculated as follows:

$$d_{i,j}^{M} = \sqrt{(\mathbf{p}_i - \mathbf{p}_j)^T C^{-1} (\mathbf{p}_i - \mathbf{p}_j)}. \tag{2.2}$$

where C^{-1} is the inverse covariance matrix of the selected point set. In this work, a covariance matrix is derived from the projected feature points. If the data points are strongly correlated, the covariance will be high. Dividing by a large covariance will effectively reduce the distance. Likewise, if the data points are not correlated, then the covariance is not high and the distance is not reduced much.

Let's study a compared example of Euclidean and Mahalanobis distance. In Table 2.1, shows the distances of four neighbor points shown in Figure 2.6 from center point $\mathbf{p}_s$ and their increasing ratios. Mahalanobis (M) and Euclidean (E) distance columns show actual distances computed by corresponding distance metric equations. and the last two columns show the ratio of distances compared to the unit of each metric; i.e., the distance from fixed points. For evaluating how points are propagated in space, the distances with another fixed point are computed. In our example, the point $\mathbf{p}_1$ is selected as a fixed point and the distance from $\mathbf{p}_1$ to center point $\mathbf{p}_s$ is considered as

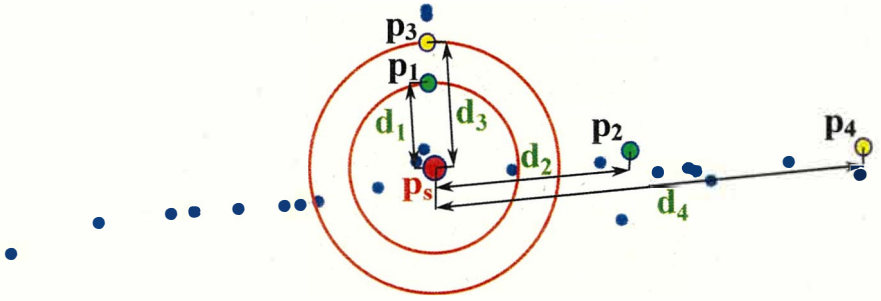

(a) Euclidean distance

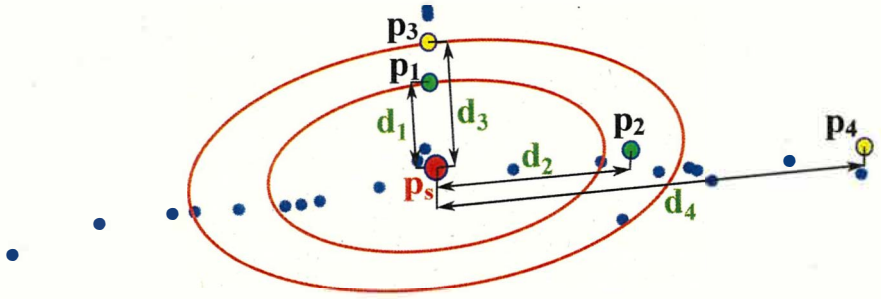

(b) Mahalanobis distance

Figure 2.6: A compared example of Euclidean distance and Mahalanobis distance.

Table 2.1: The measurement of Mahalanobis distance and Euclidean distance from the selected center point to neighbor ones.

Measuring points	Mahalanobis Distance ($d^M_{i,s}$)	Euclidean Distance ($d^E_{i,s}$)	Distance ratio ($r^M_{i,s}$)	Distance ratio ($r^E_{i,s}$)
$(\mathbf{p}_1, \mathbf{p}_s)$	1.122	0.058	1	1
$(\mathbf{p}_2, \mathbf{p}_s)$	1.174	0.125	1.046	2.128
$(\mathbf{p}_3, \mathbf{p}_s)$	2.275	0.080	2.027	1.360
$(\mathbf{p}_4, \mathbf{p}_s)$	2.296	0.155	2.045	2.638

the unit distance for each distance metric. The ratio between other distances to unit distance is calculated by Equation (2.3). This ratio shows how many distances increase compared to the unit distance.

$$r_{i,s} = \frac{d_{i,s}}{d_{1,s}} \tag{2.3}$$

From the Table 2.1, $d^E_{3,s}$ is Euclidean distance between the points $\mathbf{p}_3$ and $\mathbf{p}_s$, even it is almost twice closer to center point compared to Euclidean distance $d^E_{4,s}$ between the points $\mathbf{p}_4$ and $\mathbf{p}_s$, its increasing ratios ($r^M_{3,s}$ and $r^M_{4,s}$) are almost same in Mahalanobis distance metric. $r^M_{3,s}$ is a Mahalanobis distance ratio of points $\mathbf{p}_3$ and $\mathbf{p}_s$. $r^M_{4,s}$ is a Mahalanobis distance ratio of points $\mathbf{p}_4$ and $\mathbf{p}_s$. In other words, points $\mathbf{p}_3$ and $\mathbf{p}_4$ are located in almost the same distance in Mahalonobis space. When comparing $d^E_{2,s}$ and $d^M_{2,s}$, that point $\mathbf{p}_2$ is very close to center point by Mahalanobis distance, where $\mathbf{p}_2$ is twice far in distance compared to its own Euclidean unit. $d^E_{2,s}$ is a Euclidean distance between the points $\mathbf{p}_2$ and $\mathbf{p}_s$. $d^M_{2,s}$ is a Mahalanobis distance between the points $\mathbf{p}_2$ and $\mathbf{p}_s$.

2.5 A Recognizing Flake Surfaces of A Stone Tool

The cognitive foundations of the ancient people have increasingly studied via lithic technology over the last thirty years [30]. However, the approach and methodology of this study are not developed as a theory. Archaeology is characterized by the interdisciplinarity and the transversality of their approaches and methodologies. In this context, the study of lithic technology is necessary to use the advanced technologies of computer graphics for depict shape and three-dimensional archaeological models.

Three-dimensional technologies offer for cultural heritage preservation [42] and lithic analysis [32]. Recently, the approaches to point clouds have increased in the archaeological application. The point-cloud-based techniques of recognizing, matching, reassembling and feature line extracting have been introduced in the lithic analysis.

Today, a number of methods of matching broken fragments for archaeological research are presented. Matching methods for lithic materials work to restore broken fragments of stone tool.

Altantsetseg et al. [5] have presented a new method for pairwise matching of broken fragments. This paper introduced new descriptor for pairwise matching and additionally calculated some factors on the feature point cluster for comparing boundary points. Likewise, the most matching algorithms are calculated on the contour points of flake surfaces.

Huang et al. [22] assemble the broken object using the geometric information derived from the fracture surfaces of the fragments. This paper consists of a graph-cuts based segmentation algorithm for identifying potential fracture surfaces, feature-based robust global registration for pairwise matching of fragments, and simultaneous constrained local registration of multiple fragments.

Brown et al. [9] proposed a method based on geometry properties for matching of fresco fragments.

Yang et al. [52] proposed pairwise matching of stone tools based on the contour points and mean normals of segmented regions. Yang proposed a complete matching system of mixed lithic materials. First, the normal vectors of the points are calculated via a least-square plane fitting estimation.

Then, a region growing segmentation algorithm [44] is applied to obtain flake surfaces. When using region growing segmentation method two parameters, angle threshold of normal vector θ and curvature threshold c is used to get a superb segmentation result. The greater values of θ and c lead to a smaller number of flake surfaces. The gravel surfaces (that belong to the original rock, not to a flake surface) and the flake surfaces whose number of points is smaller than 1/20 of the original points are removed. They are not put into flake surfaces that will be matched. Next, the contour points of flake surfaces are extracted using the convex hull algorithm. After that to make pairwise matching, flake surfaces are divided into the source surface and the target surface. Each point of the source and target surfaces, two 4-point sets are constructed based on the contour points to compute the course rigid transform matrix. The distance between the point set on the source surface transformed by a rigid matrix and point set on the target surface is measured. The study considers that two points are matched when the distance is smaller than the threshold value. While their methods are useful for archaeological studies, the length of the contour line highly affects to result and this system lack to explicit segmentation method. To improve the robustness of the error metric, flake surfaces have to be precisely segmented. When using region growing segmentation method, points located on the smooth area of flake surface are merged into clusters. But points located on the edges of flake surfaces cannot be merged into one of the smooth clusters. Therefore, additional conditions are required to match the flake surfaces. The advantages of our proposed study have been to segment the precise edge of the flake surface.

The segmentation of point clouds plays a very significant role in the three-dimensional recognition system. Many researchers have tried to develop segmentation methods to obtain geometric properties by fitting curves and surfaces for point clouds. The methods proposed by Yan et al. [51] and Chen et al. [10] are suitable for a relatively flat data-type point cloud. The surface or curve fitting tasks require time and it is also difficult to extract the exact edge points because edge points are not always included in the scan data. The region growing methods classify points into homogeneous parts by similar geometric properties of points. The region growing methods, proposed by Woo et al. [48], Tovari et al. [46] and Ning et al. [34], directly segment points from unordered point clouds and these methods are faster than the above-mentioned fitting method.

High accuracy enables most segmentation methods to classify points into a new region when the difference of variables is small. As a result, many regions are created and additional analysis of combining the regions is needed to be present. Furthermore, the segmentation method is often faced with overlapping problems of edges. Through the surface complexity of stone tools, it is not enough to segment three-dimensional points just by using normal vectors and smoothness. Thus, this work presents another segmentation method that uses characteristics derived from the base drawing of a stone tool. In this research, a new feature-line-based segmentation method for unorganized point clouds is proposed.

Advantage of this method is to recognize the flake surface using both geometric and archaeological features of the stone tool. To compare the region growing segmentation method, the proposed method can extract precise edges of the flake surfaces and does not affected by the merging problem. For this purpose, we studied the scale drawing of the stone tool. The main advantage of the study of scale drawing is scale drawing covers many general concepts and principles that apply to stone tools found anywhere.

2.6 Computer Graphics Techniques Used in Lithic Analysis

As for the illustration system of stone tools, LANG Co., Ltd introduced "Stoneware PEAKIT system" into the market today. Stoneware PEAKIT is illustration system used in the archaeological application. It creates an image illustrating both geometric and archaeological features of stone tools. Stoneware PEAKIT creates a shape analyzed image of orthographic projection, multifaceted expansion generated from "CORE DATA" of stoneware measured at a pitch of 0.1 to 0.2 mm. This system is clearly extracting the relief information of the stone tool surface. It creates "PEAKIT" and "dimension drawing/dimension table" from delivered stoneware. Stoneware PEAKIT is a semi-automated system. To create a "CORE DATA", this system uses openness to obtain three-dimensional features of an object then combine it to the three-dimensional measurement done on the object. Thus, this system

Figure 2.7: PEAKIT image of a stone tool [26].

needs more time. Figure 2.7 shows a PEAKIT image of a stone tool by using openness [11].

A scale drawing of stone tools is time-consuming work. Our aim is to propose a different framework of three-dimensional illustration of stone tools like scale drawing, which has been enhanced to recognize with point clouds.

Chapter 3

Feature Line Extraction of Stone Tools Based on Mahalanobis Distance Metric

3.1 Overview of The Chapter

This chapter detailed the feature line extraction algorithm using Mahalanobis distance metric for stone tools. First, feature point and feature line extraction techniques are sequentially represented. Then, the ground truth of stone tools is extracted from the scale drawing. The experiment result is shown in the result and limitation section.

3.2 Feature Extraction

To achieve our goal, three-dimensional features are extracted from the point cloud and the feature lines are constructed using the features. To draw the base drawing, specialist divides it into several layers. Commonly, the layer of the outline is first drawn and the layer of ridge lines are drawn later. In this work, consequently, the outline is extracted first and ridge lines are extracted later.

3.2.1 Outline Extraction

The outline is extracted first in the same manner as an actual base drawing process. The outline extraction is performed using the alpha-shape of Point Cloud Library.

3.2.2 Potential Feature Point Detection

The feature lines are constructed by connecting feature points. To take the reality of feature lines, boundary points are very important. Until these days many feature point detection algorithms have been introduced. A shape of a flake surface is sometimes created by chance with hitting operation. Thus, the shape around ridge lines becomes sometimes ambiguous. Since local surface properties are suitable for detection of potential feature points, surface variation at a point is introduced. It allows us to distinguish the point which belongs to a flat or an edge point in the point cloud with low computation. To make a base drawing, ridge lines bounded by the flake surface have to be extracted. To detect the points that locate on the surface boundary, accurate surface variation is required with the underlying surface.

In our method, extraction of the potential feature point is based on Pauly et al. [40]. Measured points $\mathbf{x}_i (i = 0, ..., n)$, where i is the index of point $\mathbf{x}_i$ and $n + 1$ is the number of input points, is evaluated by surface variation σ_i^j for point $\mathbf{x}_i$ as

$$\sigma_i^j = \frac{\lambda_0}{\lambda_0 + \lambda_1 + \lambda_2} \tag{3.1}$$

where λ_0, λ_1, and λ_2 are the eigenvalues of covariance matrix C with $\lambda_0 \leqslant \lambda_1 \leqslant \lambda_2$ and j is the number of the neighborhood of point $\mathbf{x}_i$. In the experiment, the number of the neighborhood of each point was selected ($j = 10, 20, 30, ..., 200$). Using the surface variation with the different number of the neighborhood has the advantage to reduce the noise.

To detect potential feature points, the surface variation on every point is calculated with the various number of neighbors. After the calculation, every point $\mathbf{x}_i$ obtains a set of surface variations $(\sigma_i^{10}, \sigma_i^{20}, \sigma_i^{30}, ..., \sigma_i^{200})$. If all surface variations σ_i^j are greater than given threshold ε, the point $\mathbf{x}_i$ is determined the potential feature point $\mathbf{p}_y^c$ $(y = 0, ..., m)$, where $m + 1$ is the number of potential feature points, as shown in the following Eq.(3.2). In other words, if above-mentioned condition is satisfied, point $\mathbf{x}_i$ can be noted $\mathbf{p}_y^c$ because of

$\mathbf{p}_y^c = \mathbf{x}_i$. Moreover, surface variation σ_i^j of $\mathbf{p}_y^c$ can be noted σ_y^j. Otherwise, that point is not assumed to the potential feature point.

$$\begin{cases} \mathbf{p}_y^c & \text{if all } \sigma_y^j \text{ is satisfied } \varepsilon < \sigma_y^j \\ \mathbf{O} & \text{other} \end{cases} \tag{3.2}$$

The sphere radius is used to detect neighboring points in Section 3.2.2, 3.2.3 and 3.2.4. The number of neighbors varies with each point depending on the sphere radius. The sphere radius R is defined by Eq.(3.3).

$$R = a \cdot \overline{d} \tag{3.3}$$

where a is a scale value of iteration and $\overline{d}$ is the average distance [8] between the points shown in Eq.(3.4).

$$\overline{d} = \frac{1}{n+1} \sum_{i=0}^{n} |\mathbf{x}_i - \mathbf{q}| \tag{3.4}$$

where $\mathbf{q}$ is one nearest point of $\mathbf{x}_i$, and $|\mathbf{x}_i - \mathbf{q}|$ is the distance between points $\mathbf{x}_i$ and $\mathbf{q}$.

In this work, each potential feature point $\mathbf{p}_y^c$ is attributed to corresponding surface variation and covariance matrix in order to extracting feature lines. To extract the point which is used for constructing the feature lines, the corresponding surface variation is defined for each potential feature point. To calculate the Mahalanobis distance, the inverse covariance matrix is calculated on each potential feature point.

Since every $\mathbf{p}_y^c$ needs to one corresponding surface variation, the corresponding surface variation of potential feature points $\mathbf{p}_y^c$ is evaluated by the maximum surface variation of a set of surface variations. After the evaluation, every point $\mathbf{p}_y^c$ obtains one corresponding surface variation $\sigma_y^{\max}$. This method assumes that the input point cloud is a manifold surface.

The second attribute which belongs to $\mathbf{p}_y^c$ is covariance matrix C_y. Firstly the tangent plane at $\mathbf{p}_y^c$ is defined by the normal vector that is derived by the eigenvector corresponding to the minimum eigenvalue. Then the neighbor potential feature points of $\mathbf{p}_y^c$ are projected onto the tangent plane. Then the covariance matrix is constructed from the projected potential feature points. The covariance matrix C_y at selected potential feature point is defined as:

$$C_y = \frac{1}{k} \sum_{l=1}^{k} (\mathbf{p}_l^c - \overline{\mathbf{p}})^T (\mathbf{p}_l^c - \overline{\mathbf{p}}) \tag{3.5}$$

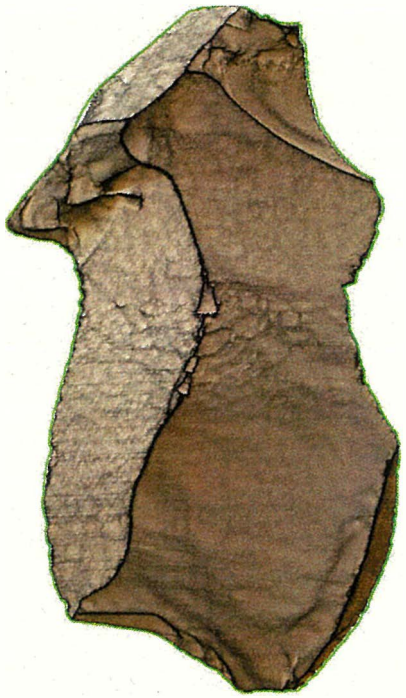

Figure 3.1: A PEAKIT image of a stone tool [11]

where k is number of neighbor projected potential feature points at $\mathbf{p}_y^c$ when a is equal to 10 and $\overline{\mathbf{p}}$ is the average point of the projected potential feature point set $\mathbf{V}_l(l = 1, ..., k)$ shown in Eq.(3.6):

$$\overline{\mathbf{p}} = \frac{1}{k}\sum_{l=1}^{k}(\mathbf{V}_l) \tag{3.6}$$

Then the inversion of covariance matrix C_i^{-1} is derived.

Figure 3.1 shows a PEAKIT image of a stone tool which is extracted feature line from three-dimensional data of an object by using openness [11]. Figure 3.2 shows the extracted outline of the stone tool. Figure 3.3 shows the potential feature points and Figure 3.4 shows the result of thinning. Finally, Figure 3.5 shows the constructed feature lines using the Mahalanobis distance. Detail of thinning process and constructing feature lines are described in Section 3.2.3 and 3.2.4.

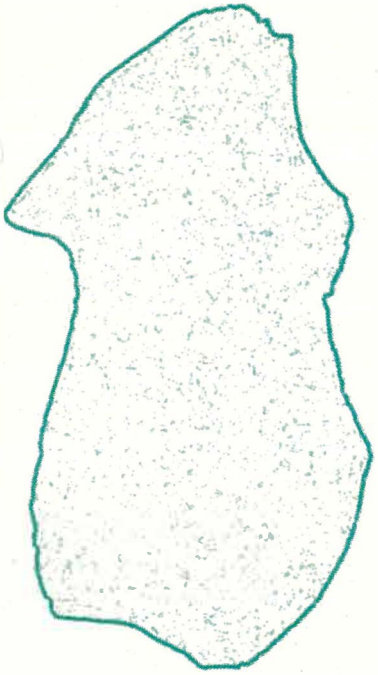

Figure 3.2: An extracted outline of the stone tool

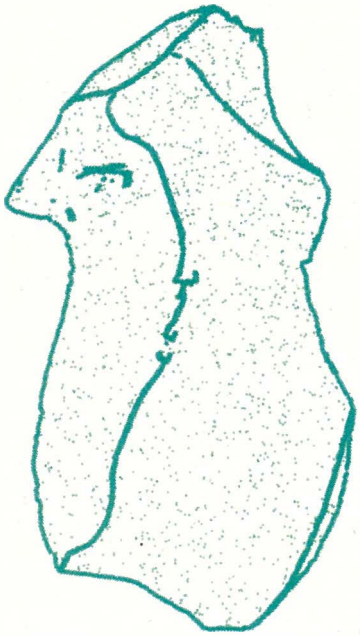

Figure 3.3: The frontal view of the potential feature points

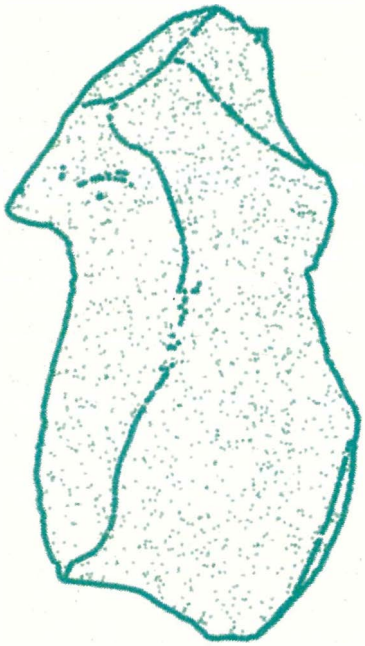

Figure 3.4: The frontal view of thinning feature points after Laplacian smoothing operation

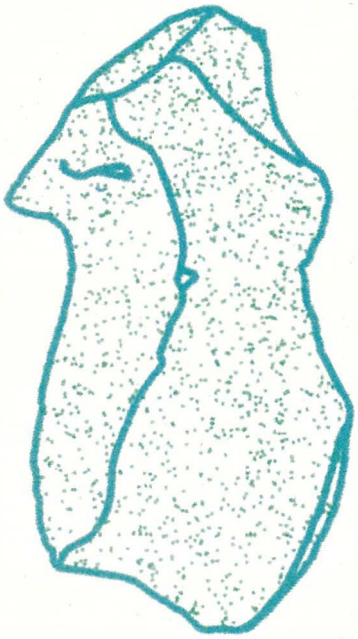

Figure 3.5: The frontal view of extracted feature lines based on Mahalanobis distance metric

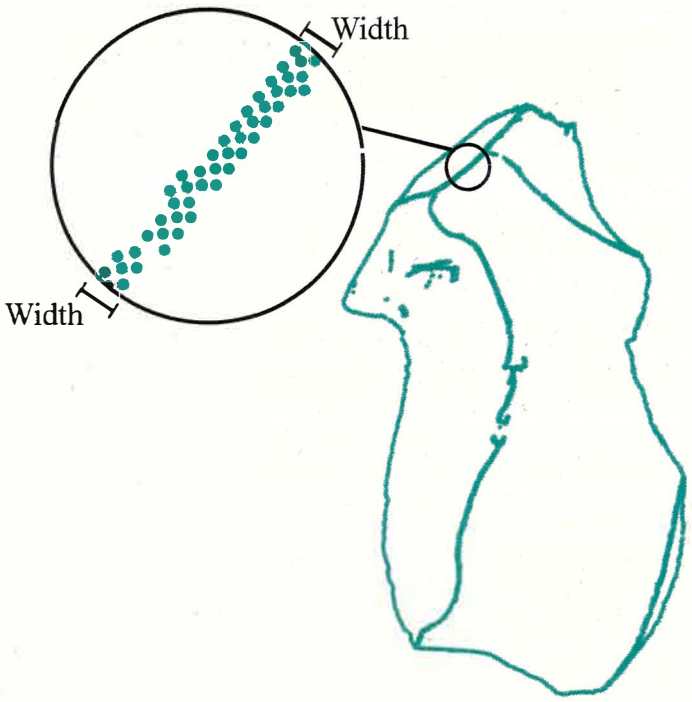

Figure 3.6: The width example of potential feature points

3.2.3 Thinning Feature Point

Potential feature points described in Section 3.2.2 have the width and the density as shown in Figure 3.6. Since our method to apply potential feature points, the amount of feature points are detected around the sharp edges in Figure 3.6. To build precise feature lines, some potential feature points are selected to the constructing feature lines. Selecting a number of potential feature points is called the thinning process in this research. The thinning process is evaluated on the only potential feature points. This section describes how to thin potential feature points.

To construct feature lines, the potential feature points have to be thinned. For this purpose, all potential feature points are thinned using a surface variation weighted Laplacian smoothing filter.

The ridge points are detected as the potential feature points. However, some potential feature points are extracted far from the real feature lines. Figure 3.7 shows an example of the far and close potential feature points. If the potential feature point is far from the feature line, the number of neighbors,

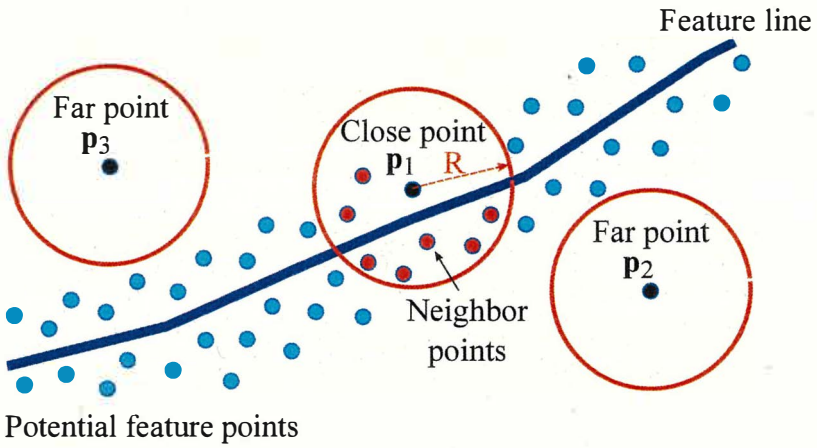

Figure 3.7: The example of the potential feature points.

which is inside of the sphere, is few. On the other hand, if the potential feature points are close to the feature line, the number of neighbors is many.

In the thinning process, some unnecessary feature points can be removed as previous situation. The remaining points that are close to the feature line will be moved closer to the feature lines. The potential feature points are thinned by the following two parts.

Part1: *Remove unnecessary potential feature points*

Step 1. Initialize $a = 5$

Step 2. Calculate number of the neighbor potential feature points v inside the sphere radius R.

Step 3. The potential feature points with less than three neighboring points are removed inside the sphere radius R.

Step 4. If no remove points this process is finished. If it is exist, goto Step 2.

In the second part, some remained potential feature points are selected to the constructing feature lines by the following iteration.

Part2: *Thinning process*

Step 1. Moving to a new position

- Initialize $a = 5$

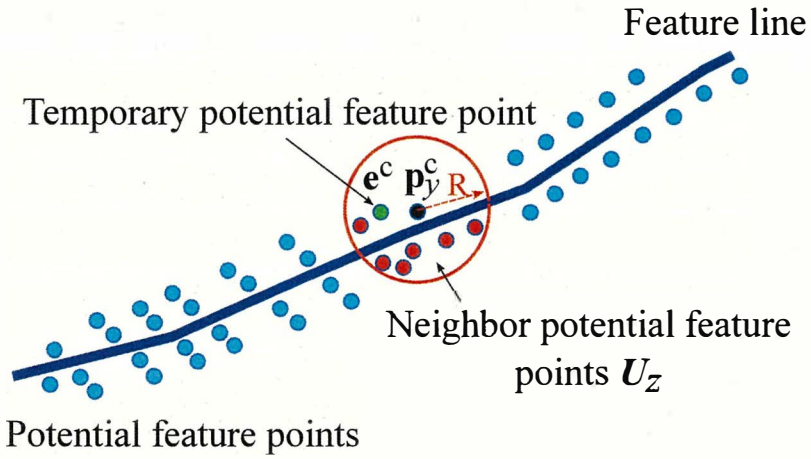

(a) Before

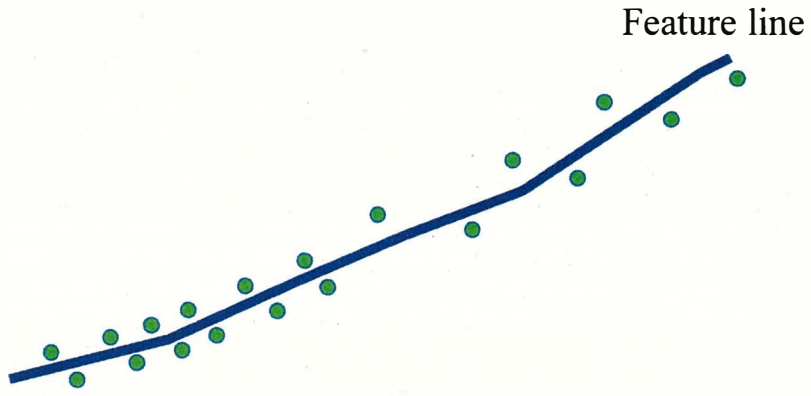

(b) After

Figure 3.8: The example of selected potential feature points with highest surface variation in neighbor potential feature points

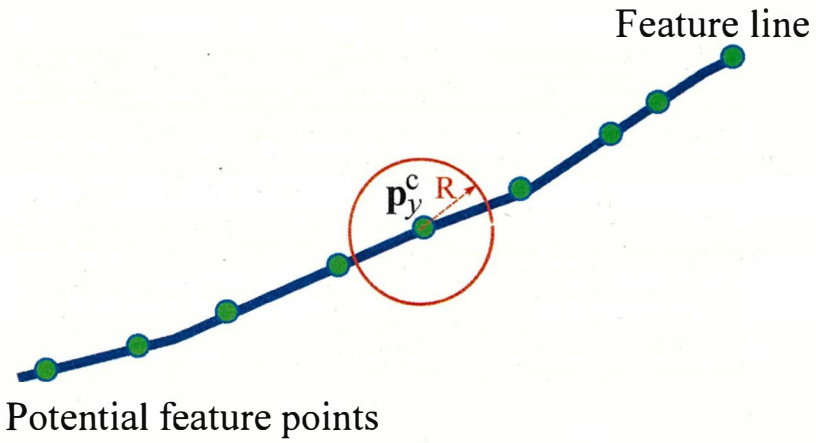

Figure 3.9: The example of final potential feature points

- Calculate number of the neighbor potential feature points v inside the sphere radius R of $\mathbf{p}_y^c$. Let $\mathbf{Q}_f(f = 1, ..., v)$ be the neighbor potential feature points.

- For the potential feature points $\mathbf{p}_y^c$, a new position $\overline{\mathbf{p}_y^c}$ is calculated by the averaging of the neighbor potential feature points by Eq.(3.7)

$$\overline{\mathbf{p}_y^c} = \frac{1}{v} \sum_{f=1}^{v} \mathbf{Q}_f \tag{3.7}$$

- All potential feature points $\mathbf{p}_y^c$ are moved to the calculated new position $\overline{\mathbf{p}_y^c}$.

Step 2. Obtaining a point with high surface variation

- Initialize $a = 0.5$

- Calculate number of the neighbor potential feature points u inside the sphere radius R of $\mathbf{p}_y^c$. Let $\mathbf{U}_z(z = 1, ..., u)$ be the neighbor potential feature points.

- Create a set $(\sigma_1^{\max}, \sigma_2^{\max}, \sigma_3^{\max}, ..., \sigma_u^{\max})$ of surface variations at each neighbor potential feature point $\mathbf{U}_z$. The corresponding surface variation which is already calculated in the previous section, is used.

- For the potential feature point $\mathbf{p}_y^c$, find the potential feature point which has the highest surface variation from a set of surface variation, as a temporary potential feature point $\mathbf{e}^c$. Figure 3.8 (a) shows the temporary potential feature point $\mathbf{e}^c$.

- For all potential feature points $\mathbf{p}_y^c$, temporary potential feature points are obtained.

Step 3. Temporary potential feature points are selected as the potential feature points for the Step 4. Other unselected potential feature points are removed. In this step, number of potential feature points will be reduced. Green points in Figure 3.8 (b) shows obtained potential feature points with high surface variation after this step is finished.

Step 4. If the new potential feature points no longer selected, the process is finished. If it is selected, goto Step 1. Figure 3.9 shows the example of final potential feature points.

The number of the thinning feature point can be controlled by the parameter of a scale value of iteration.

After the thinning process, the potential feature points are moved. Therefore, the potential feature points are shrunk to the initial position of $\mathbf{p}_y^c$. After the potential feature points are moved, we call these points are thinning feature points $\mathbf{p}_z^r(z = 0, ..., t)$, where $t + 1$ is the number of thinning feature points.

These extracted thinning feature points are selected to construct the feature lines.

Filtration steps do not significantly affect the position of the real point. Because feature point with the highest surface variation is usually detected on the edges of a stone tool.

3.2.4 Extraction of Feature Lines

In our method, the feature line extraction approach combines a Mahalanobis distance metric algorithm. Feature line construction is not an easy task for stone tools and many approaches have been proposed [21, 39, 53]. However, base drawings cannot be completely connected by using previous works.

To construct feature lines, [21, 39, 53] connect the nearest feature points one by one. As suggested in [8], the feature lines are initialized at the seed points, and arbitrary points obtained by thinning feature points can be chosen as the new seed points. To select a point on the feature line, the nearest thinning feature point should be found sequentially.

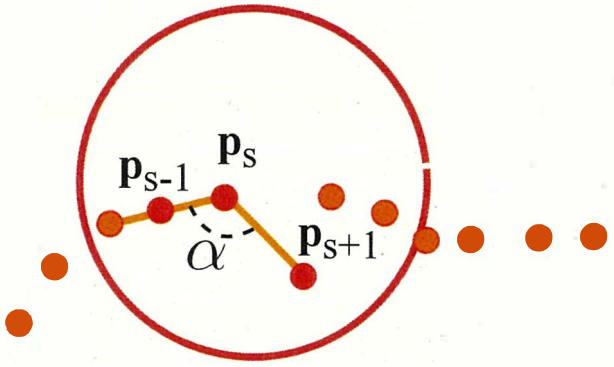

Figure 3.10: An example of constructing feature line.

This study connects thinning feature points dependent on the variation of neighboring points. Thinning feature points are selected along the principal direction. To find the nearest thinning feature point, the Mahalanobis distance metric evaluates the distances between the current seed point and its nearest thinning feature points. The distances between the current seed point $\mathbf{p}_s$ and the thinning feature points $\mathbf{p}_z^r$ are calculated by Eq. (3.8).

$$d_{z,s}^M = \sqrt{(\mathbf{p}_z^r - \mathbf{p}_s)^T C_s^{-1} (\mathbf{p}_z^r - \mathbf{p}_s)}. \tag{3.8}$$

where the inverse covariance matrix C_s^{-1} is already calculated in the section 3.2.2. Let $D_e(e = 1, ..., h)$, where h is the number of neighbor thinning feature point, be the Mahalanobis distances of the neighboring thinning feature points at $\mathbf{p}_s$. The nearest distance is found by a sorting algorithm.

The proposed feature line constructing algorithm consists of two steps. At first, feature points are connected to each other by the Mahalanobis distance metric regardless of branch. The initial seed point is selected from the beginning of thinning feature points. The degree of an angle α defined by three points such as the previously selected thinning feature point $\mathbf{p}_{s-1}$, current seed point $\mathbf{p}_s$ and a detected nearest thinning feature point $\mathbf{p}_{s+1}$, is calculated. Figure 3.10 shows the angle α between the aforementioned thinning feature points. If the α is greater than a given threshold value θ, the detected nearest thinning feature point $\mathbf{p}_{s+1}$ is added to the feature line L. In contrast, the detected angle α is lower than a given threshold value θ, the next nearest thinning feature point $\mathbf{p}_{s+2}$ is checked.

$$L = \begin{cases} \mathbf{p}_{s+1} & \text{if } \alpha \text{ is satisfied } \alpha \geq \theta \\ \mathbf{p}_{s+2} & \text{otherwise} \end{cases} \tag{3.9}$$

To construct feature lines, the satisfied thinning feature point $\mathbf{p}_{s+1}$ should be selected as a new seed point $\mathbf{p}_s$ based on the Mahalanobis distance.

Second, the distinct feature lines are connected to each other. Endpoints of the distinct feature lines are connected to the nearest feature point located on the nearest feature line by the Mahalanobis distance metric.

3.3 Results

3.3.1 Making Ground Truth Image of Base Drawing

One improvement of this study is we tried to identify the similarity of extracted base drawing and ground truth. Moreover, we try to evaluate the accuracy of our proposed method. To do the evaluation, some detailed analysis and preconditions must be made. In this thesis, all evaluations between ground truth and extracted base drawing are based on overlapping pixels. For that approximation, Cole et al. [13] mentioned simple and robust pixels based evaluation method and they also mentioned the practical reasons for this application.

One important step of evaluating similarity and accuracy is to support the ground truth of base drawing. The ground truth of base drawing is created by the method described in [13] to be the most accurate. The ground truth image of base drawing and an image of the extracted base drawing are quantified into the same size image.

Based on Cole et al. [13], the ground truth image of base drawing is made by the following steps. Initially, the image of the base drawing created by a specialist is converted to a grayscale image. Then, the converted grayscale image segmented into two regions by Otsu's method. Otsu's method (discriminant analysis method) is one of the methods that automatically decides the threshold and performs binarization processing. After that, the pixel width is defined using the real size of the stone tool. In the experiment, the one-pixel width is quantified of $0.1mm$. Next binarization image is thinned by the iterated thinning process. The iterated thinning process is used to narrowing the line widths of several pixels into the width of one pixel [13]. Figures (3.11 - 3.16) show the extracted ground truth image of stone tools.

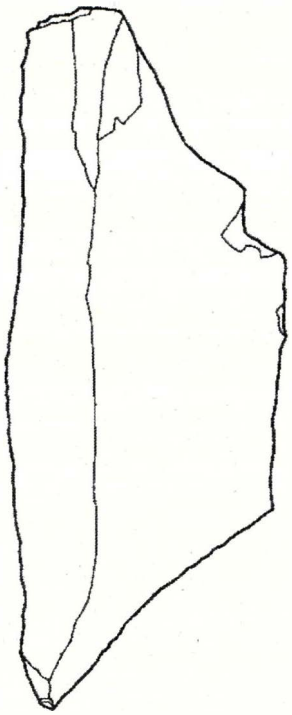

Figure 3.11: The extracted ground truth image of Stone tool 1.

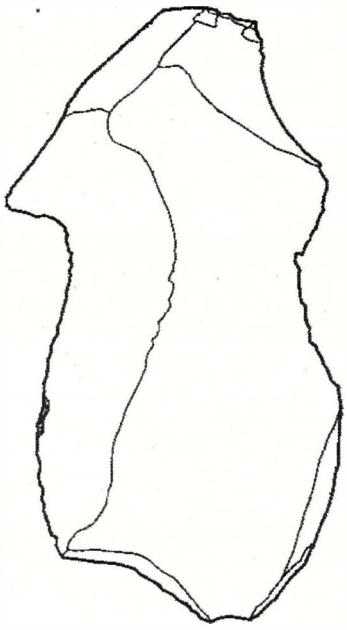

Figure 3.12: The extracted ground truth image of Stone tool 2.

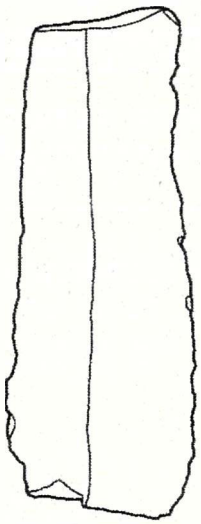

Figure 3.13: The extracted ground truth image of Stone tool 3.

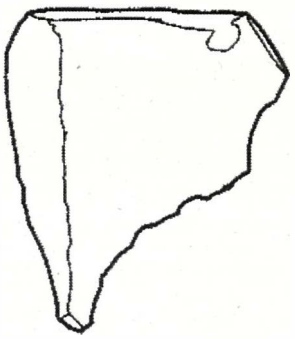

Figure 3.14: The extracted ground truth image of Stone tool 4.

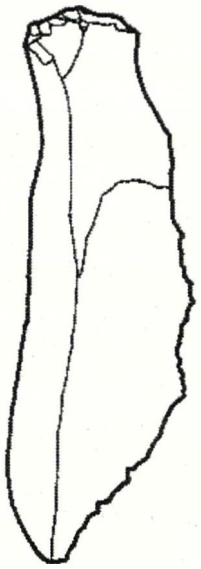

Figure 3.15: The extracted ground truth image of Stone tool 5.

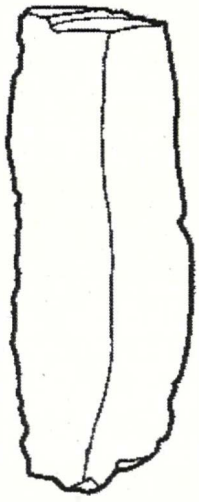

Figure 3.16: The extracted ground truth image of Stone tool 6.

To compare three-dimensional feature lines and a two-dimensional image of the base drawing, extracted base drawings are required to capture in the two-dimensions. Then, the two-dimensional image of extracted base drawings is compared to the ground truth image of the base drawing.

The first challenge in this study is to define the drawn viewpoint of the base drawing. For the base drawing, the specialist makes measurement and define the drawing viewpoint of the stone tool. In this study, the extracted feature lines are rotated in all three directions with a wide range. To find the precisely drawn viewpoint of base drawing, each rotated feature lines are captured. The correspondence between the captured feature line image and ground truth image of base drawing is made on pixels in every iteration. The viewpoint of base drawing is defined by rotation angle with the highest correspondence. After a viewpoint is set, the extracted base drawing is rotated and captured via the defined viewpoint.

3.3.2 Experiment Results

This section describes the result from our experiments. The experiments were performed in an Intel Core i7-6700 CPU 3.40 GHz machine with 8GB of RAM and Intel(R) HD Graphics 530. We used the Point Cloud Library (PCL). The input data is point data of stone tools obtained by four-directional 3D laser scanners [6].

This thesis automatically extracts a base drawing of stone tools. The stone tools are evaluated on the front pose. We tested our proposed method on the six actual stone tools. The extracted base drawings of the stone tools are shown in Figures (3.17 - 3.18). In these figures, the first left column shows the scale drawing and the second column shows the base drawing which is referred to as ground truth. The third column shows the result of the proposed method. To reduce the working hours of creating scale drawing, this paper aims to automatically extract base drawing.

To evaluate the similarity between the ground truth of base drawing and the extracted base drawing, the approximation of pixels are measured [13]. Using the real sizes of the stone tools, the images of the ground truth and the extracted base drawing are quantified by the one-pixel width of $0.1mm$.

To show the similarity between the ground truth of base drawing and the extracted base drawing, Figure 3.19 shows the images built up on top of each

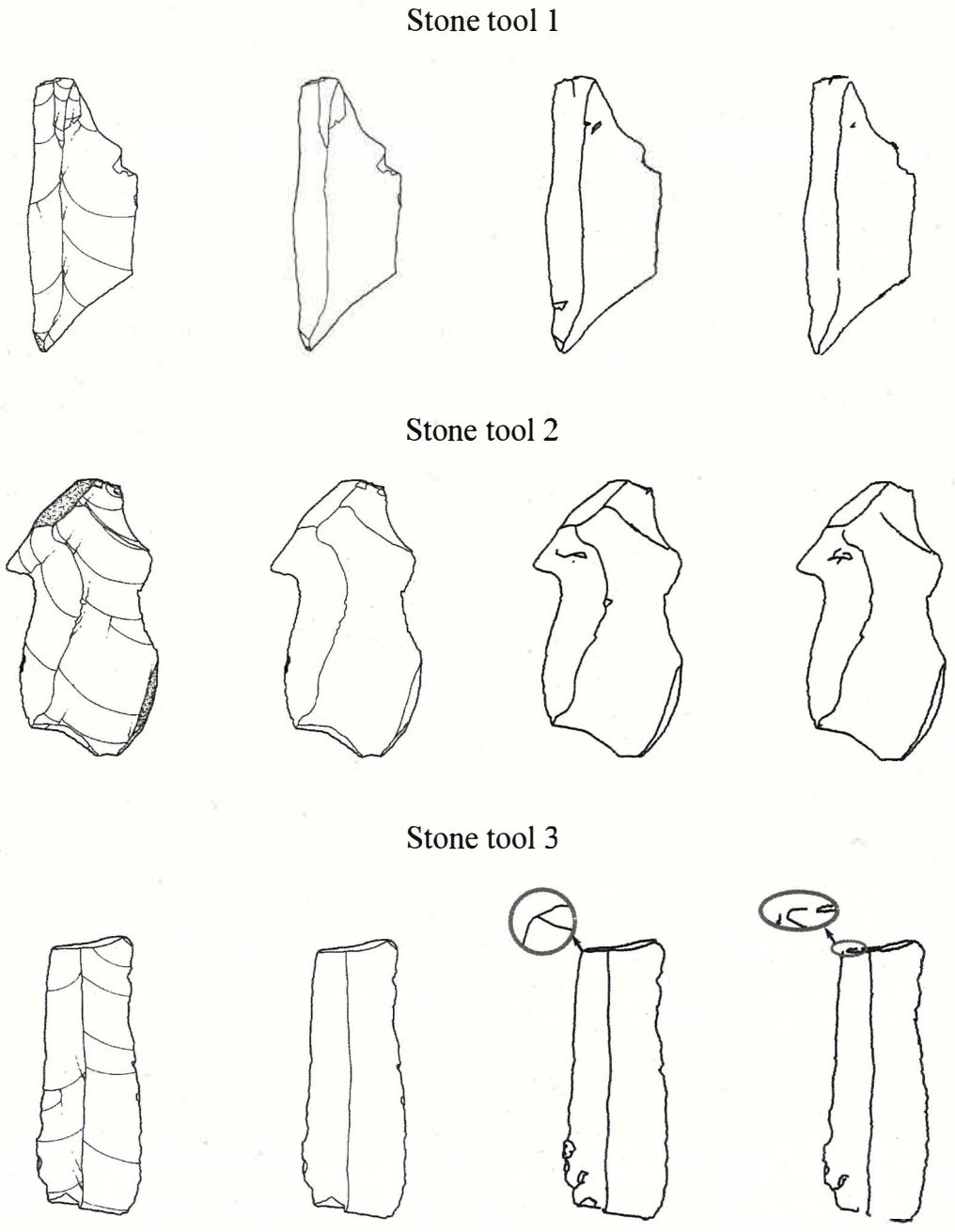

Figure 3.17: The result of the proposed method of Stone tools (1-3). The first left column shows the scale drawings of stone tools, the second column shows the ground truth of base drawings, the third column shows the results of the proposed method and fourth column shows the results of the previous work.

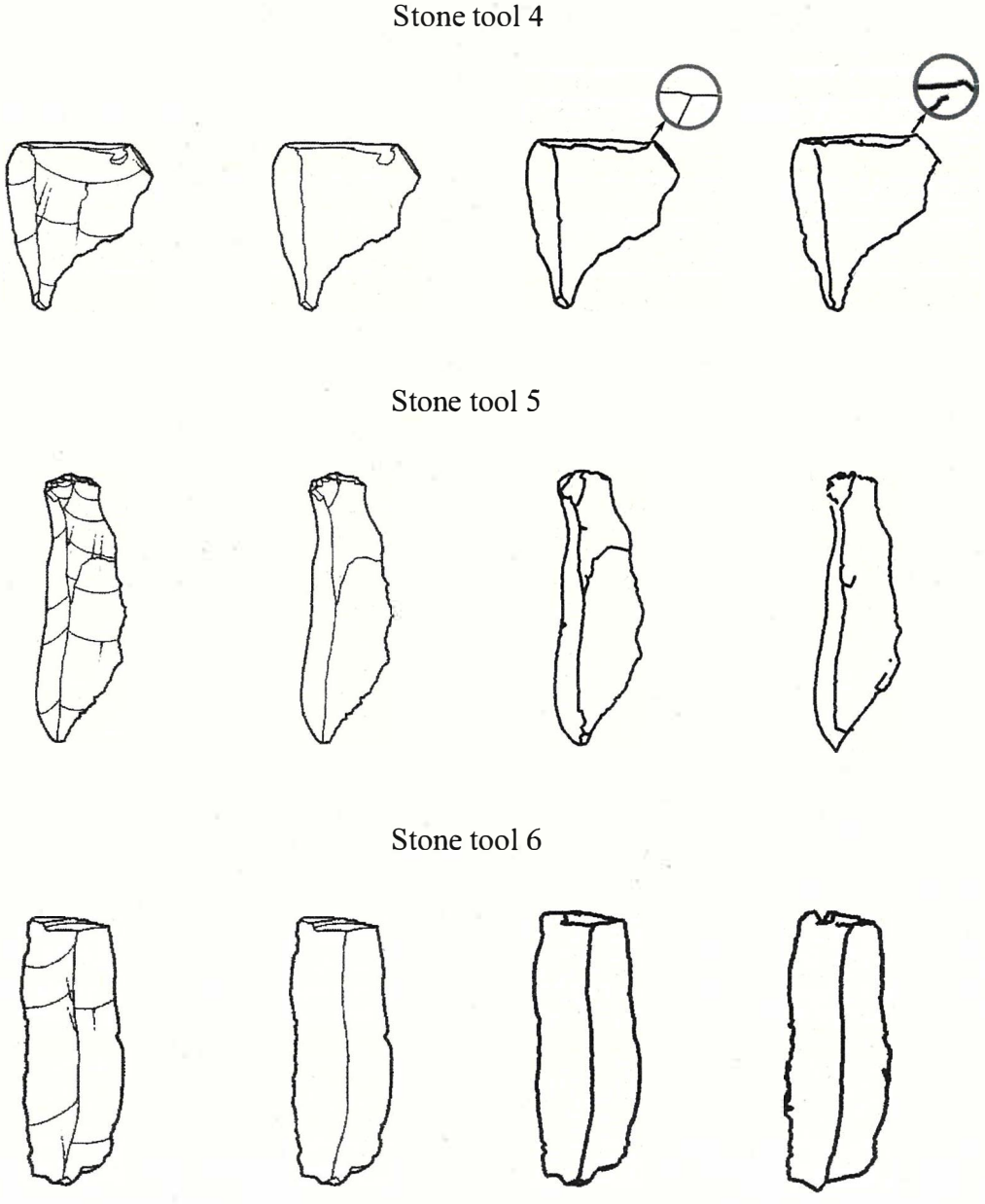

Figure 3.18: The result of the proposed method of Stone tools (4-6). The first left column shows the scale drawings of stone tools, the second column shows the ground truth of base drawings, the third column shows the results of the proposed method and fourth column shows the results of the previous work.

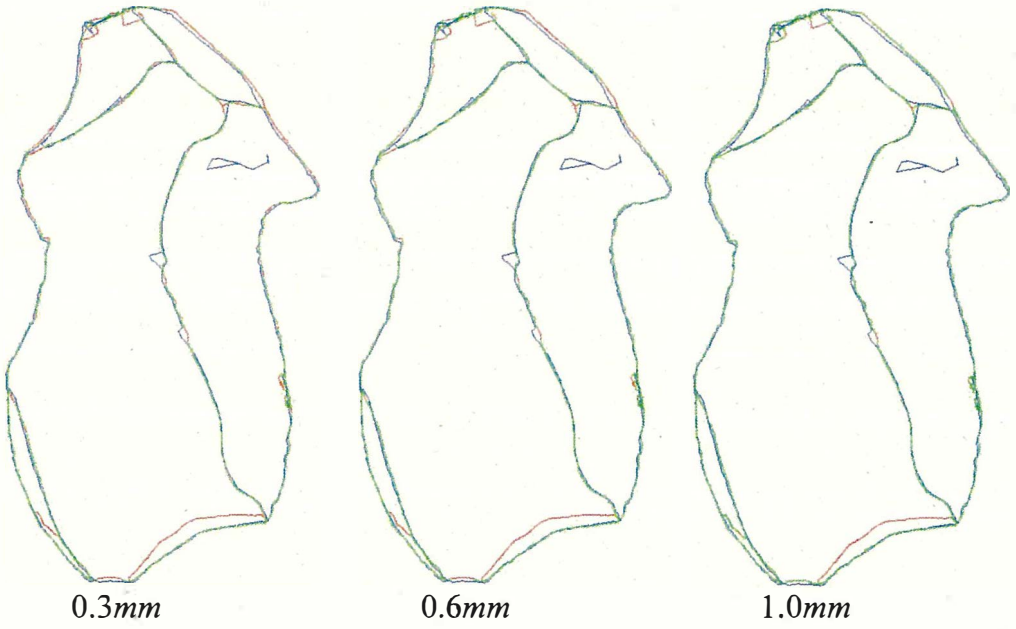

Figure 3.19: The closest pixels with various tolerance.

other and visualizes how much they close or overlap. In Figure 3.19, the closest (also overlapped OP) pixels are illustrated by green and distant pixels are illustrated by red within the tolerance of $0.3mm$, $0.6mm$ and $1mm$. Image pixels of extracted base drawings are illustrated by blue. In this example, the extracted feature lines are very close with ground truth in most areas, especially along with obvious features such as boundaries of flakes, but differ in the junction areas.

In order to quantify similarity (SL), we compute a proportion of the closest pixels OP between ground truth (GT) image and extracted base drawing an image. The quantity of similarity is defined by Equation (3.10).

$$SL = \frac{OP}{GT} \cdot 100 \tag{3.10}$$

Table 3.1 shows the number of points, physical properties of the actual stone tools and some evaluation. The similarity of the extracted base drawing and ground truth is defined in the distance of $0.5mm$.

To define whether the manually created base drawing can be replaced with the automatically extracted base drawing is possible, extracted base drawing and hand-drawn base drawing are compared quantitatively. To measure the extraction accuracy, F1 score, the harmonic average of the precision (PC) and

Table 3.1: Physical size of stone tools and evaluations

Measured stone tools	Points	Stone tool sizes			Similarity	Average distance (mm)	F1 score
		Height (mm)	Length (mm)	Width (mm)			
1	174393	80.4	31.8	8.1	83.126	0.403	0.876
2	201679	72.5	44.1	10.8	82.373	0.410	0.899
3	144306	68.0	25.2	7.7	94.885	0.402	0.930
4	46469	29.2	25.6	5.1	87.872	0.397	0.925
5	52913	48.8	15.3	4.2	78.028	0.416	0.813
6	45230	37.2	14.1	4.0	87.343	0.412	0.904

recall (PR), is evaluated in each stone tool data where the F1 score reaches its best value at 1 and worst score at 0.

The precision has defined by the ratio of the closest pixels and pixels of the extracted base drawing image (EL). The recall has defined by the ratio of the closest pixels and pixels of ground truth image. Equations (3.11,3.12) shows the equation of precision and recall. We define "close" by choosing a distance of $0.1mm$ to $0.6mm$. Figure 3.20 shows the F1 scores of the extracted feature lines for all six stone tools.

$$PC = \frac{OP}{EL} \tag{3.11}$$

$$PR = \frac{OP}{GT} \tag{3.12}$$

Figure 3.20 shows the F1 scores of the extracted base drawing for all six stone tools. The best value at 1 of the F1 score indicates that the extracted base drawing is the same as the ground truth, and the extracted base drawing can be reduce working hours of manually creating a base drawing. F1 score takes

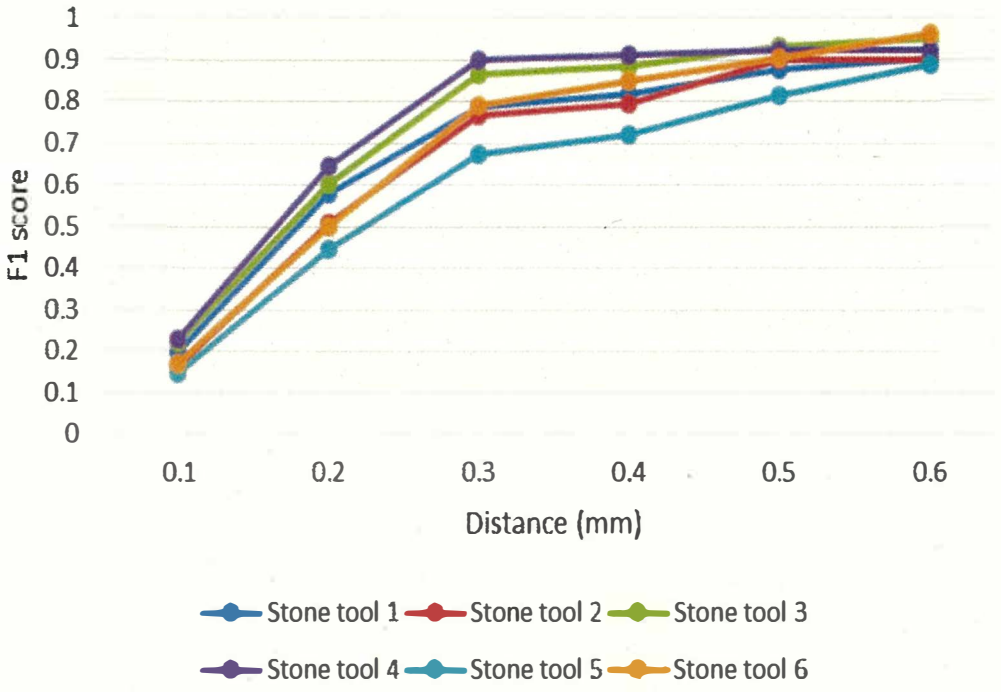

Figure 3.20: Graph of F1 score of extracted lines.

both false negative and false positive pixels into account. False-negative pixels express undetected edges from the ground truth. False-positive pixels express unnecessary edges of the extracted base drawing in Figure 3.21(a).

Moreover, average distance d' is measured by Eq.(3.13).

$$d' = \frac{\sum_{i=0}^{n} w_i d_i}{\sum_{i=0}^{n} w_i} \tag{3.13}$$

where w_i is the overlapped pixel within the distance d_i. The average distance is measured between the distance 0.1mm to 0.6mm within a step 0.1. The result of average distance is shown in Table 3.1.

We introduced the comparison of automatically extracted base drawing and ground truth images. The base drawing of ground truth is drawn by hand and the proposed base drawing is extracted from the point cloud. When using the Euclidean distance metric, feature lines constructed by the previous method shown in the fourth column of Figures (3.17 - 3.18) cannot be fully constructed and a lot of gaps between feature lines. Some unconnected edges

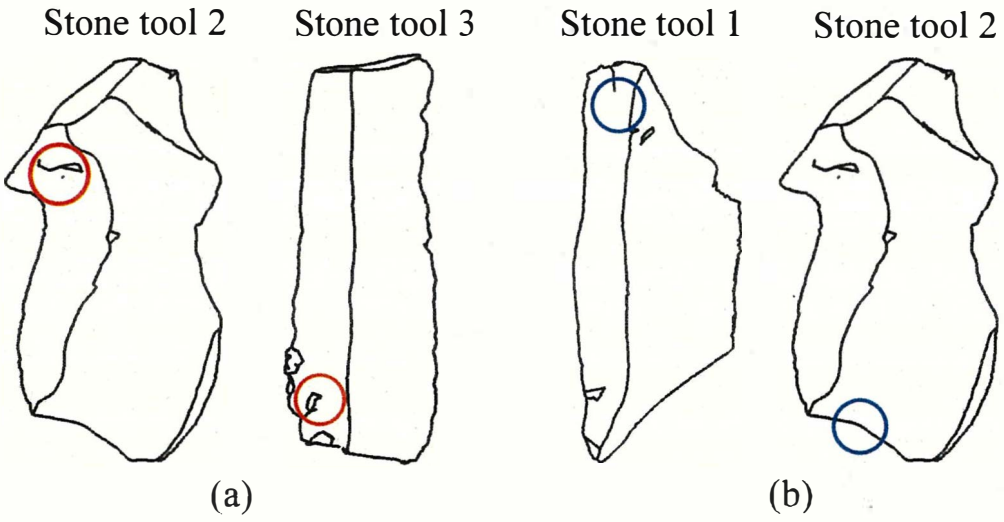

Figure 3.21: The unnecessary edges and undetected edges of the results.

with hard to see are enlarged in Figures (3.17 - 3.18). Moreover, some feature lines are unextracted. Our proposed method can extract closed base drawing and the edges are completely connected. Figures (3.17 - 3.18) show the result of completely connected edges which is enlarged and cannot be connected by the previous method. In the experiment, the similarities of the stone tools are between 78.028 to 94.885. Our method can properly extract long ridge lines. The average distances of extracted base drawings are between 0.397 to 0.416 in all six stone tools.

3.4 Limitation

Figure 3.22 shows the types of ridge lines in a scale drawing. The limitation of our method is that it is difficult to extract corner small ridge lines of a stone tool. The corner small ridge lines need more specialist knowledge because the shapes around small ridges are ambiguous. The small ridge lines are magnified in Figure 3.22.

The unnecessary ridge lines are extracted in the stone tools 2 and 3 shown in Figure 3.21(a) and some referenced ridge lines are not extracted in the stone tool 1 and 2 shown in Figure 3.21(b). In these cases, extracting ambiguous ridge lines are hardly extracted by the geometric approach. In such a case,

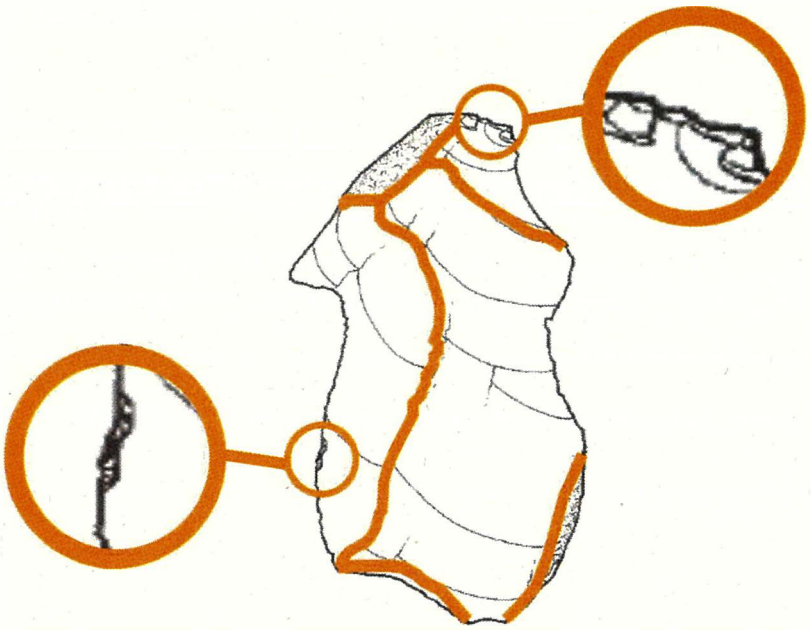

Figure 3.22: Types of the ridge lines

an archaeologist may help to extract small ridge lines.

3.5 Conclusion

In this Chapter, a novel method of the extracting base drawing is proposed. The main idea of the method is to select a candidate point of feature lines by its Mahalanobis distance. The advantage of our method is that Mahalanobis distance can reference the covariance of the local neighbor set. For stone tools, the feature lines are usually lined up. In such a manner, the Mahalanobis distance metric can extract feature lines more properly than the Euclidean distance metric for stone tools.

Chapter 4

Recognizing Flake Surfaces Based on Feature Lines of Stone Tool

4.1 Overview of The Chapter

The main idea of the Chapter is to introduce feature-line-based segmentation method. The comparison results of the proposed segmentation method and the region growing segmentation method are shown in the result section.

4.2 Feature-line-based Segmentation Method

One of the most important steps for reassembly of a stone tool is recognition of flake surfaces because the reassembly process is based on segmented flake surfaces of stone tools. Lithic material is widely used for refitting flakes of stone tools in archaeology. It is an issue to extract flake surfaces with high accuracy for matching three-dimensional fragments. Stone tools have very complicated shapes since they have many different surfaces such as flake scare, cortex, core, hatchure lines, ripples, etc. These surfaces occur during the long-term storage or by human hands.

The study of stone tool analyzes the surface edges and illustrates the scale drawing of stone tools. It is easier to assemble the surfaces by using its geometric properties such as outline and ridge line.

The region growing segmentation method is used for extracting flake surfaces whose shapes are inaccurate. This thesis introduces an algorithm for automatic recognition of the flake surfaces from point clouds. The flake surface recognition method is very effective for stone tools because it is based on the geometric characteristic of stone tools. It is possible to extract flake surfaces more accurately by using the feature lines. The proposed method based on feature lines can be highly accurate.

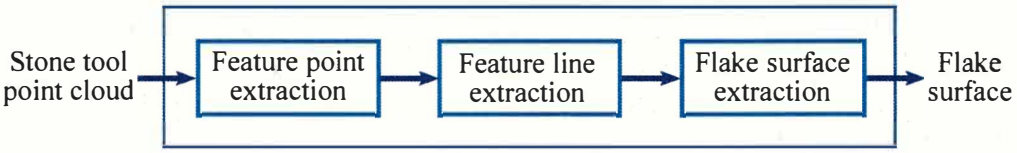

Figure 4.1: Overview of the flake surface recognition study

Figure 4.1 shows the overview of the flake surface recognition study. First, local surface features are calculated from point clouds. Then, ridge lines and outlines are extracted by using our previous work introduced in Chapter 3. After that, the flake surfaces of a stone tool are segmented based on feature lines. In this step, each point on the flakes is examined by some defined criteria of the distance and intersection.

Foremost, the surface normal of every point $\mathbf{p}_i$ in the point cloud is calculated. Surface normal $\mathbf{N}_i$ at point $\mathbf{p}_i$ is estimated from neighbor points. Practically, points are surrounded by feature line segments. Then, every point $\mathbf{p}_i$ obtains a set of distances. The distance d_i between $\mathbf{p}_i$ and a close feature line segment L is defined as the shortest distance between a fixed point and any point on the feature line segment. A distance is the length of the line segment that is perpendicular to L and passes through $\mathbf{p}_i$. Every point obtains the nearest distance from the set of distances by using the sorting algorithm. After that, a point located furthest from the feature line segment is calculated.

The proposed feature-line-based segmentation method is based on the seeded-region method. Initially, the furthest point from the feature line segment is selected for seed point $\mathbf{p}_s$. Then, $\mathbf{p}_s$ clusters its neighbor points by the following two criteria. First, neighbor points of $\mathbf{p}_s$ are calculated. To

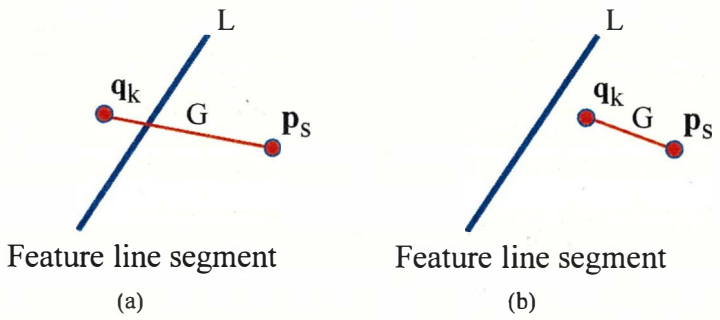

Figure 4.2: The intersection of line segments.

save the program processing speed, a distance threshold is used. If distance d_i of selected neighbor point $\mathbf{q}_k$ is greater than given threshold value υ, $\mathbf{q}_k$ is clustered to the seed point region. Second, if $\mathbf{q}_k$ is located near the feature line, local coordinate system x', y', z' is constructed along the normal vector of $\mathbf{p}_s$. In this case, $O'z'$ axes are upward to the normal vector of $\mathbf{p}_i$. Then, line G is constructed by $\mathbf{p}_s$ and $\mathbf{q}_k$. If line G does not intersect with nearest feature line segment L on the local coordinate system, $\mathbf{q}_k$ is segmented into the seed point region. If line segments intersect with each other on the local coordinate system, $\mathbf{q}_k$ is selected to a new seed point and the new region is created.

4.3 Results

Figure 4.3 (a) shows the initial model of the stone tool. (b) shows the base drawing of the stone tool, (c) shows the extracted feature lines of the stone tool using the Mahalanobis distance, (d) shows the result of the region growing segmentation method, and (e) shows the result of the proposed feature-line-based segmentation method. The red points shown in the result of region growing segmentation are not merged points of flake surfaces. If the thickness of these points can be reduced, there is the advantage of lowering the matching error.

The number of the original point clouds and the number of points in the three most common groups are shown in Table 4.1. Three most common groups are shown in Figure 4.4. The number of points in group 1 segmented by the proposed method is 16835 greater than that segmented by the region

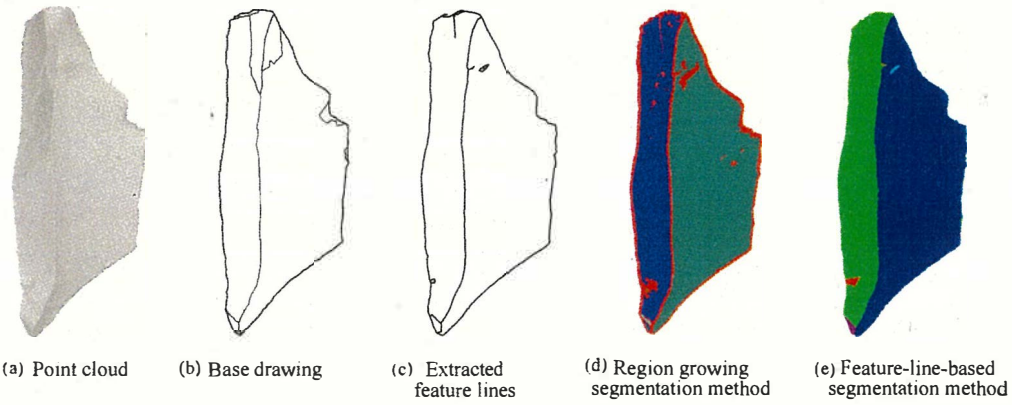

Figure 4.3: The proposed pipeline of the recognizing flake surfaces from point cloud.

growing segmentation method. Similarly, the number of points in groups 2 and 3 are 10488 and 10398 greater. Identically, the segmented area extracted by the proposed method is larger than the area extracted by the region growing method. The boundary points are subtler in the feature-line-based segmentation method.

The segmentation of the stone tool is not an easy task because of the region border accuracy problems. The region growing segmentation method is used for extracting flake surfaces however shapes of the segmented region are inaccurate. The comparison result of the proposed method and region growing segmentation method are shown in Figures (4.5 - 4.12). To evaluate the accurate shape of segmented flakes, we compare the extracted points of each flake surface. The number of points which are segmented by the proposed methods is greater than the number of points which are segmented by the region growing segmentation method. Tables (4.2 - 4.9) show the number of original point cloud and the number of points in three most common groups in 8 sample tools. The proposed flake surface extraction method based on feature lines is high accuracy for the region border. The shapes of the segmented region for both methods are similar. But the boundary points are more subtle in the proposed method.

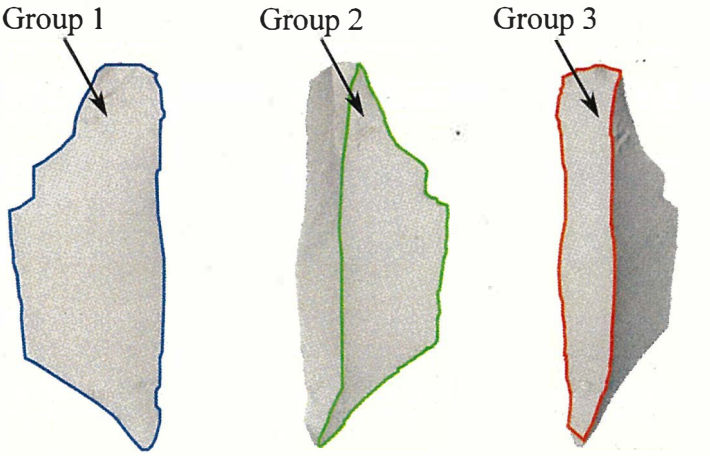

Figure 4.4: The most common segmented groups.

Table 4.1: Number of the original points and segmented parts.

Methods	Region growing segmentation method	Feature-line-based segmentation method	Difference between the segmented groups
Type of the model	Flake	Flake	
Number of points	349756	349756	
Group 1	156271	173106	16835
Group 2	104226	114714	10488
Group 3	46588	56986	10398

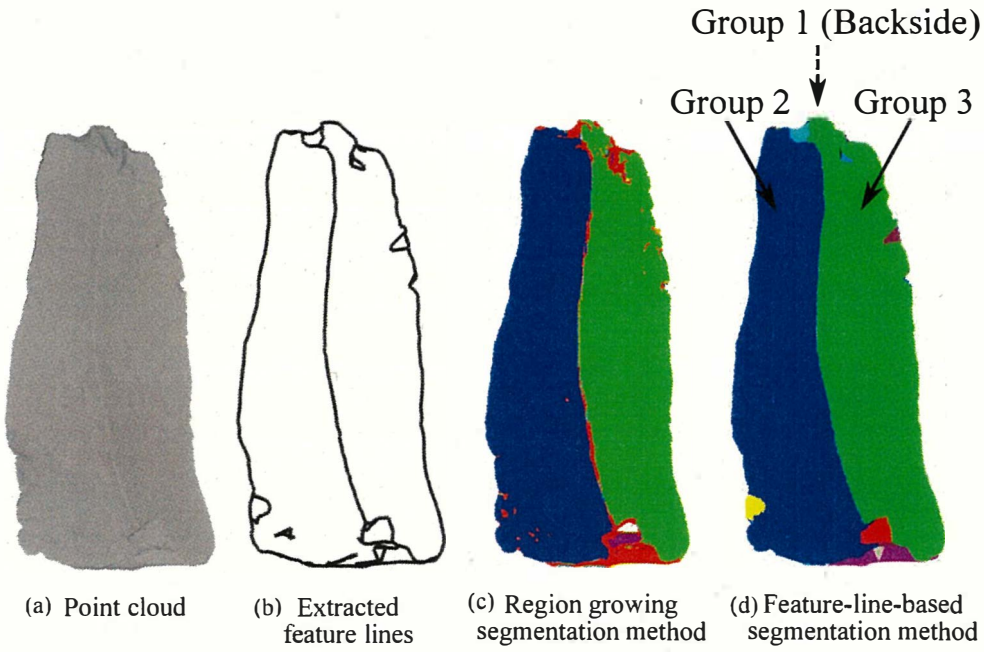

Figure 4.5: Sample tool 1: Comparison result of feature-line-based segmentation method.

Table 4.2: Sample tool 1: Number of the original points and segmented parts.

Methods	Region growing segmentation method	Feature-line-based segmentation method	Difference between the segmented groups
Type of the model	Flake	Flake	
Number of points	221207	221207	
Group 1	99703	109817	10114
Group 2	47363	56124	8761
Group 3	41807	49792	7985

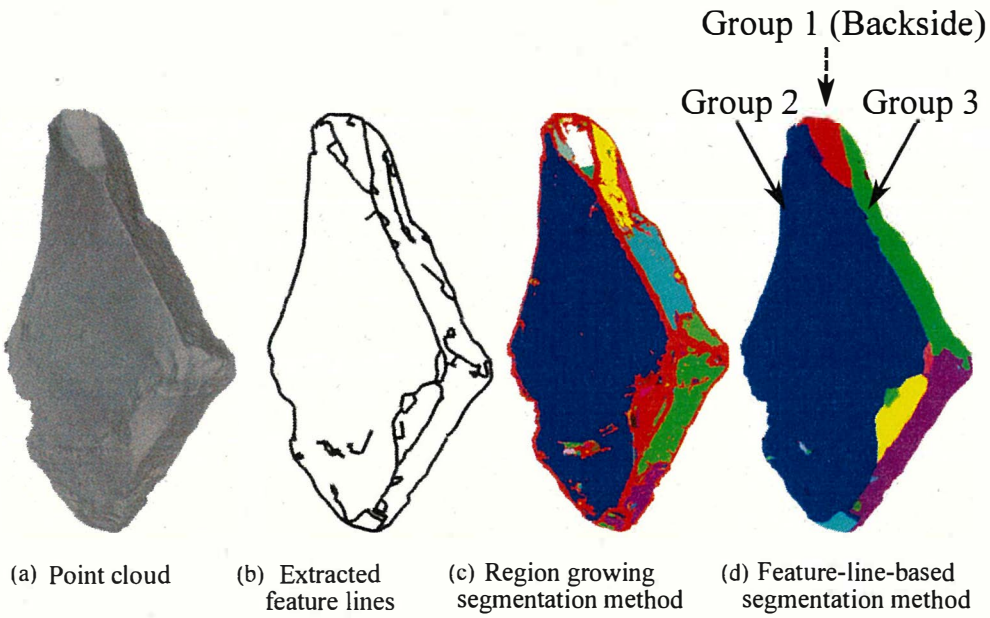

Figure 4.6: Sample tool 2: Comparison result of feature-line-based segmentation method.

Table 4.3: Sample tool 2: Number of the original points and segmented parts.

Methods	Region growing segmentation method	Feature-line-based segmentation method	Difference between the segmented groups
Type of the model	Flake	Flake	
Number of points	259449	259449	
Group 1	107601	126639	19038
Group 2	75321	85603	10282
Group 3	6725	17596	10871

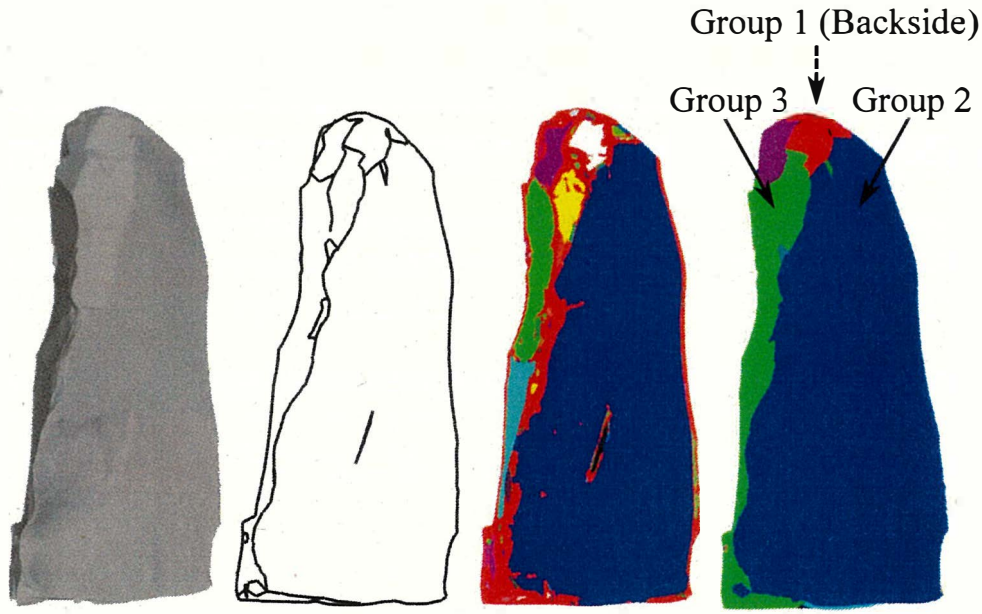

Figure 4.7: Sample tool 3: Comparison result of feature-line-based segmentation method.

Table 4.4: Sample tool 3: Number of the original points and segmented parts.

Methods	Region growing segmentation method	Feature-line-based segmentation method	Difference between the segmented groups
Type of the model	Flake	Flake	
Number of points	175868	175868	
Group 1	79288	86502	7214
Group 2	61934	68309	6375
Group 3	3686	13398	9712

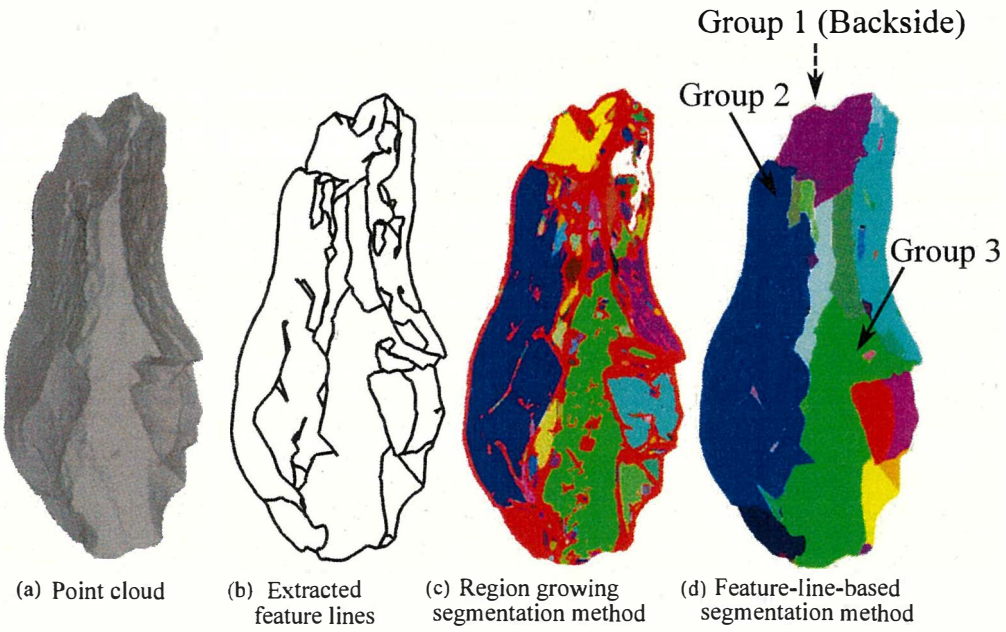

Figure 4.8: Sample tool 4: Comparison result of feature-line-based segmentation method.

Table 4.5: Sample tool 4: Number of the original points and segmented parts.

Methods	Region growing segmentation method	Feature-line-based segmentation method	Difference between the segmented groups
Type of the model	Flake	Flake	
Number of points	170085	170085	
Group 1	74431	83379	8948
Group 2	22141	28329	6188
Group 3	11553	17584	9031

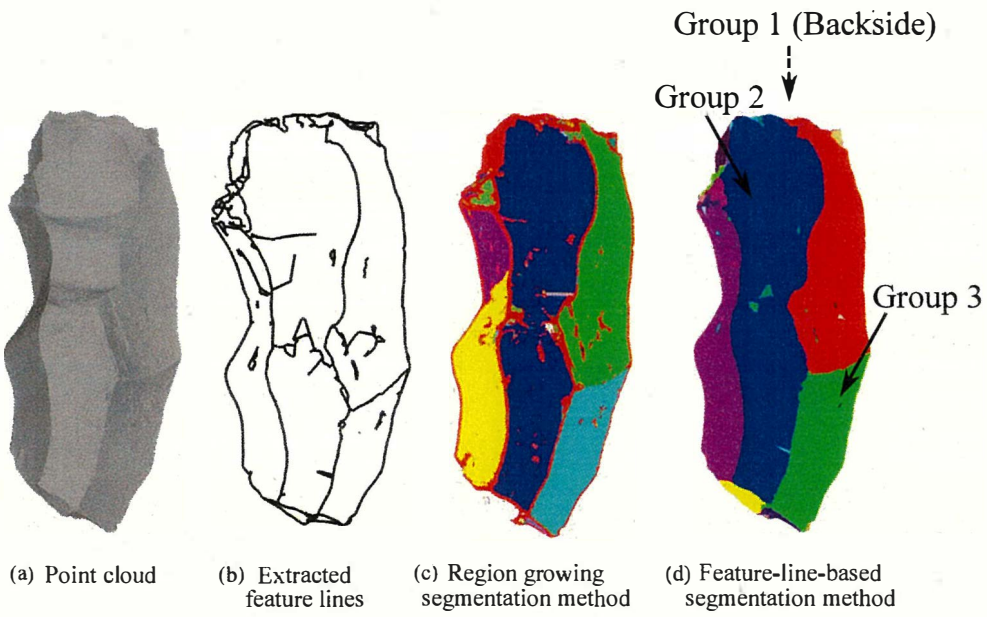

Figure 4.9: Sample tool 5: Comparison result of feature-line-based segmentation method.

Table 4.6: Sample tool 5: Number of the original points and segmented parts.

Methods	Region growing segmentation method	Feature-line-based segmentation method	Difference between the segmented groups
Type of the model	Flake	Flake	
Number of points	730716	730716	
Group 1	341104	360725	19621
Group 2	125379	144614	19235
Group 3	72737	82854	10117

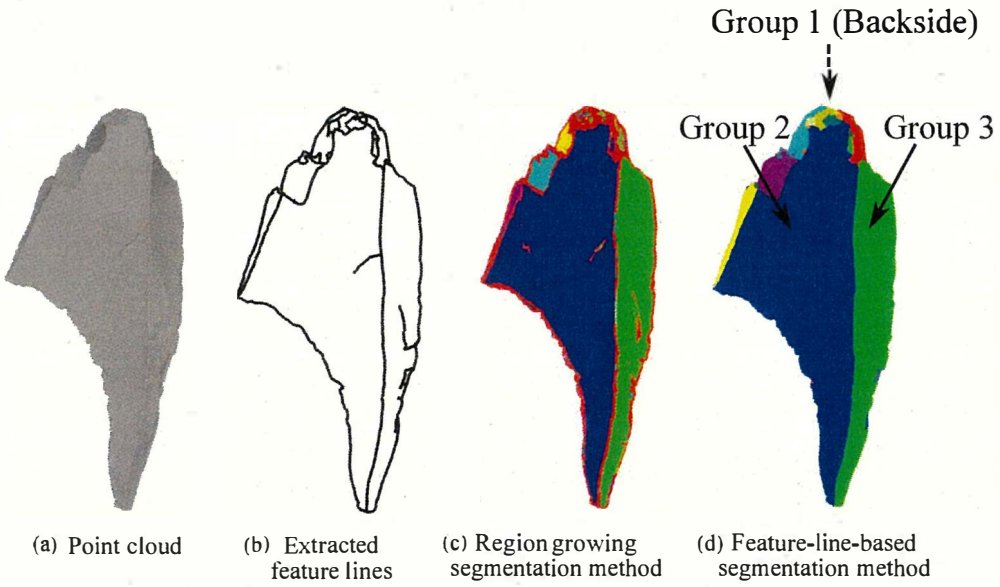

Figure 4.10: Sample tool 6: Comparison result of feature-line-based segmentation method.

Table 4.7: Sample tool 6: Number of the original points and segmented parts.

Methods	Region growing segmentation method	Feature-line-based segmentation method	Difference between the segmented groups
Type of the model	Flake	Flake	
Number of points	400961	400961	
Group 1	177984	196916	18932
Group 2	120210	131330	11120
Group 3	39914	48111	8197

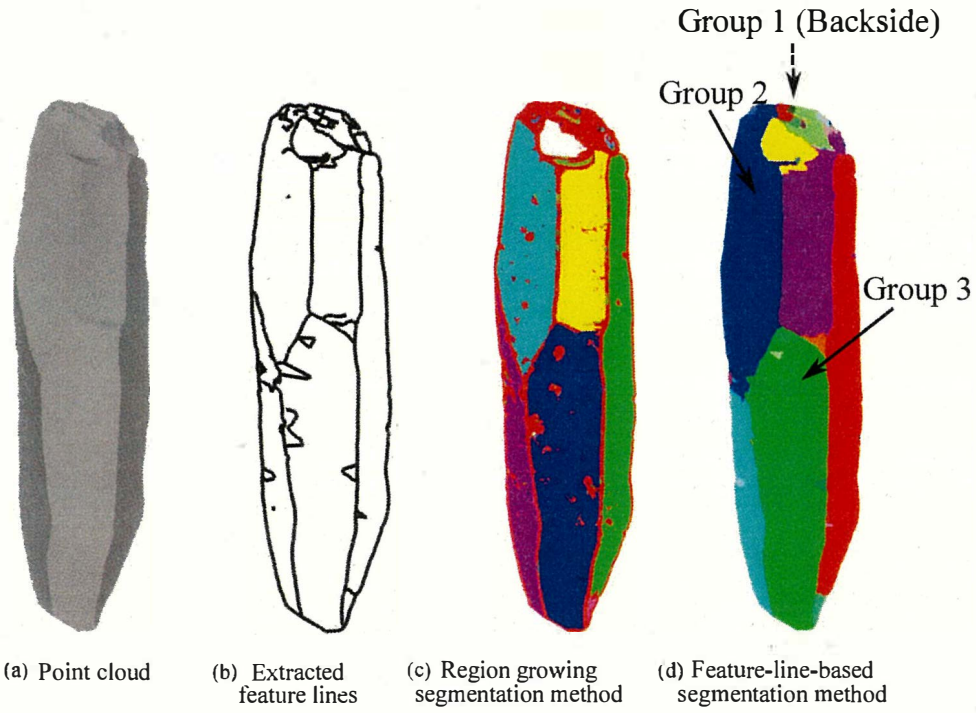

Figure 4.11: Sample tool 7: Comparison result of feature-line-based segmentation method.

Table 4.8: Sample tool 7: Number of the original points and segmented parts.

Methods	Region growing segmentation method	Feature-line-based segmentation method	Difference between the segmented groups
Type of the model	Flake	Flake	
Number of points	528093	528093	
Group 1	239001	258135	19134
Group 2	69826	77508	7682
Group 3	42001	49885	7884

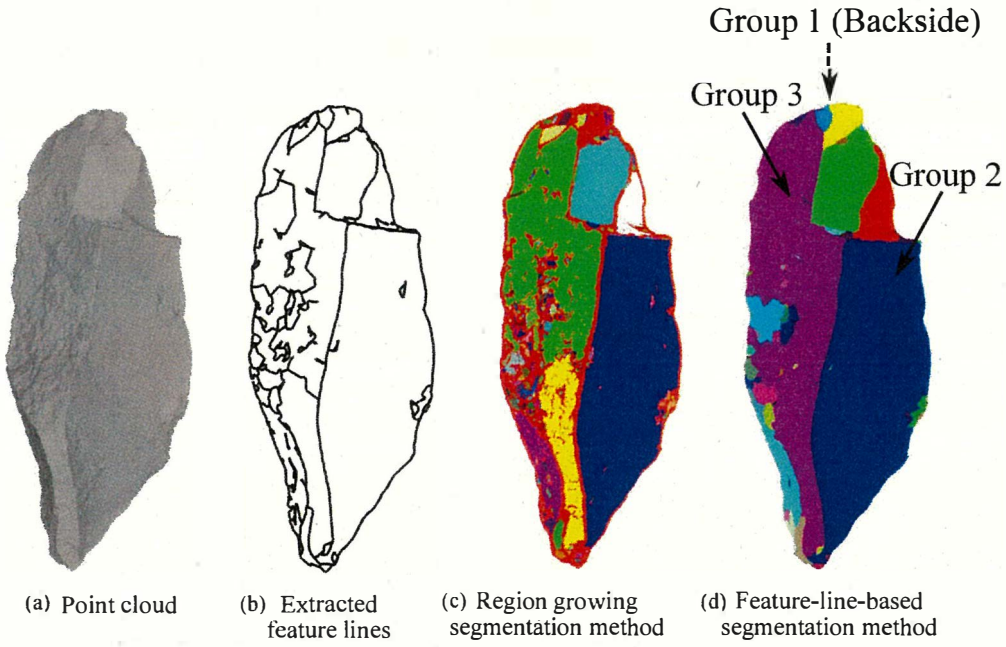

Figure 4.12: Sample tool 8: Comparison result of feature-line-based segmentation method.

Table 4.9: Sample tool 8: Number of the original points and segmented parts.

Methods	Region growing segmentation method	Feature-line-based segmentation method	Difference between the segmented groups
Type of the model	Flake	Flake	
Number of points	518313	518313	
Group 1	230695	256993	26298
Group 2	104629	113473	8844
Group 3	41785	80328	38543

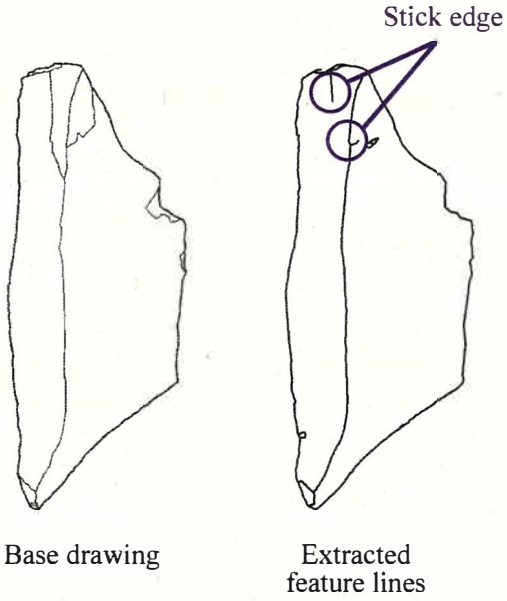

Figure 4.13: Stick edges

4.4 Limitation

When extracting feature lines, the one limitation is that some feature lines are not extracted and not entirely closed like base drawing. These unextracted edges are called stick edges are shown in Figure 4.13. In our method, if there is a not line intersection between the points, those points are merged into the one cluster. In other words, if points are surrounded by the feature lines, these points are considered the one cluster. Thus stick edges have not influenced the cluster in this method. This study does not consider stick edges.

4.5 Conclusion

This chapter presented an algorithm of automatic recognition of flake surfaces from point clouds. The flake surface recognition method is very effective for stone tool analysis because it is based on the fundamental characteristic of stone tools. The surface bounded by ridge lines can be removed and as a result, the flake surface can be recognized.

Chapter 5

Conclusion and Future Work

5.1 Conclusions

Nowadays, computer graphics and three-dimensional technology are widely used in archaeological and cultural heritage. In this thesis, we studied two topics; extracting feature lines of the stone tool and recognizing flake surfaces of the stone tool.

Chapter 1 presented the background of the point cloud and the importance of lithic materials.

Chapter 2 presented related work of the state-of-the-art introduced in digital technologies applied to archaeology and cultural heritage, the archaeological illustrating system introduced in the market and our previous approach.

Chapter 3 introduced the feature line extraction algorithm using Mahalanobis distance metric for stone tools. Moreover, efficient feature point detection method and the thinning method are introduced. Furthermore, we evaluated the similarity and accuracy of extracted feature lines and scale drawing. In addition, we tried to extract the ground truth of stone tools from the scale drawing. Because Mahalanobis distance can refer to the covariance of the local neighbor set, feature lines can be easily constructed along the main principal axis. Considering the similarity and accuracy, our proposed method can assist the archaeological illustration.

Chapter 4 presented an algorithm of automatic recognition of flake surfaces from point clouds. The proposed feature-line-based segmentation method is

very effective for stone tool analysis because it is based on the fundamental characteristic of stone tools. Our flake surface recognition method has efficiency. Because extracted flake surfaces have more accurate shape than region growing segmentation method.

5.2 Future Work

Drawing the junctions of lines in the scale drawing has difficulty. To define the junctions always needs special knowledge in archaeological application. Thus, the junction of lines is difficult to define by only programming. In future study, the proposed feature line extracting method will be improved by using illustrator tools.

Moreover, in future work, the proposed flake surface recognizing method will be applied to the process of pairwise matching of stone tools and recognition of flake surfaces of massive stone tools.

Bibliography

[1] Lithic analysis. `https://en.wikipedia.org/wiki/Lithic_analysis`.

[2] Lucile R. Addington. *Lithic illustration: drawing flaked stone artifacts for publications*. University of Chicago Press, 1986.

[3] Iwate Cultural Promotion Agency. *Orose Iseki Excavation report (in Japanese))*. 2013.

[4] Joseph Ahn, Moonseo Park, Hyun-Soo Lee, Sung Jin Ahn, Sae-Hyun Ji, Kwonsik Song, and Bo-Sik Son. Covariance effect analysis of similarity measurement methods for early construction cost estimation using case-based reasoning. *Automation in Construction*, 81:254–266, 2017.

[5] Enkhbayar Altantsetseg, Katsutsugu Matsuyama, and Kouichi Konno. Pairwise matching of 3d fragments using fast fourier transform. *The Visual Computer*, 30(6-8):929–938, 2014.

[6] Enkhbayar Altantsetseg, Yuta Muraki, Fumito Chiba, and Kouichi Konno. 3d surface reconstruction of stone tools by using four-directional measurement machine. *International Journal of Virtual Reality*, 10(1):37–43, 2011.

[7] Enkhbayar Altantsetseg, Yuta Muraki, Katsutsugu Matsuyama, Fumito Chiba, and Kouichi Konno. Feature extraction and modification for illustrating 3d stone tools from unorganized point clouds. *The Journal of Art and Science*, 12(1):36–47, 2013.

[8] Enkhbayar Altantsetseg, Yuta Muraki, Katsutsugu Matsuyama, and Kouichi Konno. Feature line extraction from unorganized noisy point clouds using truncated fourier series. *The Visual Computer*, 29(6-8):617–626, 2013.

[9] Benedict J Brown, Corey Toler-Franklin, Diego Nehab, Michael Burns, David Dobkin, Andreas Vlachopoulos, Christos Doumas, Szymon Rusinkiewicz, and Tim Weyrich. A system for high-volume acquisition and matching of fresco fragments: Reassembling theran wall paintings. In *ACM transactions on graphics (TOG)*, volume 27, page 84. ACM, 2008.

[10] Jie Chen and Baoquan Chen. Architectural modeling from sparsely scanned range data. *International Journal of Computer Vision*, 78(2-3):223–236, 2008.

[11] Fumito Chiba and Shin Yokoyama. New method to generate excavation charts by openness operators. In *Proceedings of the 22nd CIPA Symposium, Kyoto, Japan*, volume 1115, page 15, 2009.

[12] Fumito Chiba, Shin Yokoyama, Akihiro Kaneda, and Kouichi Konno. Development of network-type archaeological investigation system. *The International Archives of Photogrammetry, Remote Sensing and Spatial Information Sciences*, 40(5):99, 2015.

[13] Forrester Cole, Aleksey Golovinskiy, Alex Limpaecher, Heather Stoddart Barros, Adam Finkelstein, Thomas Funkhouser, and Szymon Rusinkiewicz. Where do people draw lines? *Communications of the ACM*, 55(1):107–115, 2012.

[14] Joel II Daniels, Linh K Ha, Tilo Ochotta, and Claudio T Silva. Robust smooth feature extraction from point clouds. In *Shape Modeling and Applications, 2007. SMI'07. IEEE International Conference on*, pages 123–136. IEEE, 2007.

[15] Joel Daniels Ii, Tilo Ochotta, Linh K Ha, and Cláudio T Silva. Spline-based feature curves from point-sampled geometry. *The Visual Computer*, 24(6):449–462, 2008.

[16] Kris Demarsin, Denis Vanderstraeten, Tim Volodine, and Dirk Roose. Detection of closed sharp edges in point clouds using normal estimation and graph theory. *Computer-Aided Design*, 39(4):276–283, 2007.

[17] Shurentsetseg Erdenebayar, Katsutsugu Matsuyama, and Kouichi Konno. Feature line extraction of stone tool based on mahalanobis distance metric. In *NICOGRAPH 2017*, pages 9–16, 2017.

[18] Shachar Fleishman, Daniel Cohen-Or, and Cláudio T Silva. Robust moving least-squares fitting with sharp features. *ACM transactions on graphics (TOG)*, 24(3):544–552, 2005.

[19] Markus Gross and Hanspeter Pfister. *Point-based graphics*. Elsevier, 2011.

[20] Stefan Gumhold, Xinlong Wang, and Rob S MacLeod. Feature extraction from point clouds. In *IMR*. Citeseer, 2001.

[21] Huy Tho Ho and Danny Gibbins. Multi-scale feature extraction for 3d models using local surface curvature. In *Computing: Techniques and Applications, 2008. DICTA'08. Digital Image*, pages 16–23. IEEE, 2008.

[22] Qi-Xing Huang, Simon Flöry, Natasha Gelfand, Michael Hofer, and Helmut Pottmann. Reassembling fractured objects by geometric matching. *ACM Transactions on Graphics (TOG)*, 25(3):569–578, 2006.

[23] Evangelos Kalogerakis, Derek Nowrouzezahrai, Patricio Simari, and Karan Singh. Extracting lines of curvature from noisy point clouds. *Computer-Aided Design*, 41(4):282–292, 2009.

[24] Shinpei Kato and Toshiaki Tsurumaru. *Sekki nyoumon jiten sandoki (in Japanese)*.

[25] Soo-Kyun Kim. Extraction of ridge and valley lines from unorganized points. *Multimedia tools and applications*, 63(1):265–279, 2013.

[26] LTD. LANG CO. Peakit image. `http://www.lang-co.jp/index.html`.

[27] Kai Wah Lee and Pengbo Bo. Feature curve extraction from point clouds via developable strip intersection. *Journal of Computational Design and Engineering*, 3(2):102–111, 2016.

[28] Marc Levoy, Kari Pulli, Brian Curless, Szymon Rusinkiewicz, David Koller, Lucas Pereira, Matt Ginzton, Sean Anderson, James Davis, Jeremy Ginsberg, et al. The digital michelangelo project: 3d scanning of large statues. In *Proceedings of the 27th annual conference on Computer graphics and interactive techniques*, pages 131–144. ACM Press/Addison-Wesley Publishing Co., 2000.

[29] Yuan Lin, Matsuyama Katsutsugu, Chiba Fumito, and Konno Kouichi. A study of feature line extraction and closed frame structure of a stone tool from measured point cloud. In *Proceedings of NICOGRAPH International 2016*. IEEE CPS, 2016.

[30] Robert Allen Mahaney. Lithic analysis as a cognitive science: A framework. *Lithic Technology*, 39(3):173–189, 2014.

[31] K. Matsufuji and S. Monta. *Yoku wakaru koukogaku (Understand archeology)*, pages 18–18. Minerva Shobo, Kyoto, JP, 2010.

[32] Paula Monteiro. Computer graphics in archaeology.

[33] Jianhui Nie. Extracting feature lines from point clouds based on smooth shrink and iterative thinning. *Graphical Models*, 84:38–49, 2016.

[34] Xiaojuan Ning, Xiaopeng Zhang, Yinghui Wang, and Marc Jaeger. Segmentation of architecture shape information from 3d point cloud. In *Proceedings of the 8th International Conference on Virtual Reality Continuum and its Applications in Industry*, pages 127–132. ACM, 2009.

[35] April Nowell and Iain Davidson. *Stone tools and the evolution of human cognition*. University Press of Colorado Boulder, 2010.

[36] George H Odell. *Lithic analysis*. Springer Science & Business Media, 2012.

[37] Hokkaido-World Heritage Jomon Remains Promotion Office. Jomon culture. `https://jomon-japan.jp/en/jomon-cultur/`.

[38] Xufang Pang, Mingyong Pang, and Zhan Song. Extracting feature curves on point sets. *International Journal of Information Engineering and Electronic Business*, 3(3):1, 2011.

[39] Xufang Pang, Zhan Song, and Wuyuan Xie. Extracting valley-ridge lines from point-cloud-based 3d fingerprint models. *IEEE computer graphics and applications*, 33(4):73–81, 2013.

[40] Mark Pauly, Markus Gross, and Leif P Kobbelt. Efficient simplification of point-sampled surfaces. In *Proceedings of the conference on Visualization'02*, pages 163–170. IEEE Computer Society, 2002.

[41] Mark Pauly, Richard Keiser, and Markus Gross. Multi-scale feature extraction on point-sampled surfaces. In *Computer graphics forum*, volume 22, pages 281–289. Wiley Online Library, 2003.

[42] Ruggero Pintus, Kazim Pal, Ying Yang, Tim Weyrich, Enrico Gobbetti, and Holly Rushmeier. A survey of geometric analysis in cultural heritage. In *Computer Graphics Forum*, volume 35, pages 4–31. Wiley Online Library, 2016.

[43] Sileshi Semaw. The world's oldest stone artefacts from gona, ethiopia: their implications for understanding stone technology and patterns of human evolution between 2· 6–1· 5 million years ago. *Journal of Archaeological Science*, 27(12):1197–1214, 2000.

[44] Ushakov Sergey. Region growing segmentation. `http://www.pointclouds.org/documentation/tutorials/region_growing_segmentation.php`, 2015.

[45] Dietrich Stout. Stone toolmaking and the evolution of human culture and cognition. *Philosophical Transactions of the Royal Society of London B: Biological Sciences*, 366(1567):1050–1059, 2011.

[46] D. Tóvári and Norbert Pfeifer. Segmentation based robust interpolation-a new approach to laser data filtering. *International Archives of Photogrammetry, Remote Sensing and Spatial Information Sciences*, 36(3/19):79–84, 2005.

[47] Christopher Weber, Stefanie Hahmann, and Hans Hagen. Sharp feature detection in point clouds. In *Shape Modeling International Conference (SMI), 2010*, pages 175–186. IEEE, 2010.

[48] H. Woo, E. Kang, Semyung Wang, and Kwan H Lee. A new segmentation method for point cloud data. *International Journal of Machine Tools and Manufacture*, 42(2):167–178, 2002.

[49] Shiming Xiang, Feiping Nie, and Changshui Zhang. Learning a mahalanobis distance metric for data clustering and classification. *Pattern Recognition*, 41(12):3600–3612, 2008.

[50] Eric P Xing, Michael I Jordan, Stuart J Russell, and Andrew Y Ng. Distance metric learning with application to clustering with side-information. In *Advances in neural information processing systems*, pages 521–528, 2003.

[51] Dong-Ming Yan, Wenping Wang, Yang Liu, and Zhouwang Yang. Variational mesh segmentation via quadric surface fitting. *Computer-Aided Design*, 44(11):1072–1082, 2012.

[52] Xi Yang, Katsutsugu Matsuyama, and Kouichi Konno. Pairwise matching of stone tools based on flake-surface contour points and normals. In *EUROGRAPHICS Workshop on Graphics and Cultural Heritage (2017)*. The Eurographics Association, 2017.

[53] Lin Yuan, Katsutsugu Matsuyama, Fumito Chiba, and Kouichi Konno. A study of feature line extraction and closed frame structure of a stone tool from measured point cloud. In *Nicograph International (NicoInt), 2016*, pages 44–51. IEEE, 2016.

List of Publications

- S. Erdenebayar, K. Matsuyama, K. Konno, "Feature Line Extraction of Stone Tool Based on Mahalanobis Distance Metric," *Proc. NICOGRAPH* **2017**, pp. 9–16, 2017

- S. Erdenebayar, K. Konno. "Feature Line Extraction of Stone Tools Based on Mahalanobis Distance Metric," *The Journal of the Society for Art and Science* **2019**, Vol.18, No.1, pp. 51–62.

- S. Erdenebayar, K. Konno, "A Study of Recognizing Flake Surfaces Based on Feature Lines of Stone Tool," *Proc. IWAIT-IFMIA* **2019**, pp. 9110491A-1–110491A-5, 2019